N-*O*-Isopropyl Sulfonamido-Based Hydroxamates as Matrix Metalloproteinase Inhibitors: Hit Selection and *in vivo* Antiangiogenic Activity.

Elisa Nuti,[1] Anna Rita Cantelmo,[2] Cristina Gallo,[3] Antonino Bruno,[2] Barbara Bassani,[2] Caterina Camodeca,[4] Tiziano Tuccinardi,[1] Laura Vera,[5,§] Elisabetta Orlandini,[1] Susanna Nencetti,[1] Enrico A. Stura,[5] Adriano Martinelli,[1] Vincent Dive,[5] Adriana Albini,[3,†] and Armando Rossello[1,†,]*

[1] Dipartimento di Farmacia, Università di Pisa, via Bonanno 6, 56126 Pisa, Italy.

[2] Science and Technological Park, IRCCS MultiMedica, via Fantoli 16/15, 20138 Milan, Italy.

[3] Laboratory of Translational Research, IRCCS Arcispedale Santa Maria Nuova, viale Risorgimento 80, Reggio Emilia, Italy.

[4] Division of Immunology, Transplants and Infectious Diseases, IRCCS San Raffaele, Via Olgettina 60, 20132 Milano, Italy

[5] CEA, iBiTec-S, Service d'Ingenierie Moleculaire des Proteines (SIMOPRO), CE-Saclay, 91191 Gif sur Yvette Cedex, France.

* To whom correspondence should be addressed: Armando Rossello, Dipartimento di Farmacia, Università di Pisa: phone: +39 050 2219562; e-mail: armando.rossello@farm.unipi.it.

† These authors equally contributed to the work.

§ Current Address: Laura Vera, Paul Scherrer Institute, 5232 Villigen, Switzerland

Abstract

Matrix metalloproteinases (MMPs) have been shown to be involved in tumor-induced angiogenesis. In particular, MMP-2, MMP-9 and MMP-14 have been reported to be crucial for tumor

angiogenesis and the formation of metastasis, thus becoming attractive targets in cancer therapy. Here, we report our optimization effort to identify novel *N*-isopropoxy-arylsulfonamide hydroxamates with improved inhibitory activity toward MMP-2, MMP-9 and MMP-14 with respect to the previously discovered compound **1**. A new series of hydroxamates was designed, synthesized and tested for their anti-angiogenic activity using in vitro assays with human umbilical vein endothelial cells (HUVECs). A nanomolar MMP-2, MMP-9 and MMP-14 inhibitor was identified, compound **3**, able to potently inhibit angiogenesis in vitro and also in vivo in the matrigel sponge assay in mice. Finally, X-ray crystallographic and docking studies were conducted for compound **3** in order to investigate its binding mode to MMP-9 and MMP-14.

1. Introduction

Angiogenesis is the formation of new blood vessels from preexisting ones and it is an essential feature of tissue remodeling associated with physiological (i.e. wound healing) and pathological processes (i.e. solid tumor growth, rheumatoid arthritis, psoriasis). In particular, tumor-induced angiogenesis is considered to be important to support growth of solid tumors to the size when they become invasive and able to give metastasis[1]. Without this process of neovascularization tumors remain in their dormant form, where proliferation is balanced with apoptosis[2]. Tumor-induced angiogenesis requires degradation of the vascular basement membrane and remodeling of the extracellular matrix (ECM) in order to allow endothelial cells to migrate and invade the surrounding tissue.

Matrix metalloproteinases (MMPs) or matrixins are a family of 23 zinc-containing endopeptidases that catalyze the cleavage of various components of the ECM. Given their ability to degrade the ECM, MMPs involvement in tumor-induced angiogenesis has been extensively investigated. Several studies[3] have shown that MMPs are involved in the “angiogenic switch”, one of the first stages in tumor growth and progression, and also in the maintenance of the growing vascular bed. Among all MMPs, MMP-2[4], MMP-9[5] and MMP-14[6] have been shown to be crucial for tumor

angiogenesis and the formation of metastasis. MMP-14 or membrane-type matrix metalloproteinase-1 (MT1-MMP) is particularly important because besides cleaving many substrates in the ECM, including type I collagen, it is also involved in MMP-2 activation on the surface of invasive tumor cells. These actions combined make this membrane-bound MMP essential to promote pericellular proteolysis and invasion[7]. The importance of MMP-14 as target in cancer therapy has been recently validated by a study from Dyax Corporation which used a highly selective fully human MMP-14 inhibitory antibody (DX-2400) in a xenograft model of human breast cancer expressing high levels of MMP-14 (MDA-MB-231)[8]. The selective inhibition of MMP-14 was able to block tumor growth, to reduce tumor vascularization and to retard the formation of metastasis.

Synthetic MMP inhibitors (MMPIs) have been proposed as suitable antiangiogenic agents to be used in cancer therapy, often in combination with cytotoxic drugs, over the last fifteen years. The first clinical trials using MMPIs in cancer treatments were largely disappointing due to the fact that most trials were conducted on patients with advanced stage disease, when the tumor vasculature was already well-established, and to the fact that broad-spectrum MMPIs were used[9]. Nowadays it is widely accepted that selective inhibitors of only those MMPs validated as targets in anticancer therapy (i.e. MMP-2, MMP-9 and MMP-14) should be used in order to have efficacy and to avoid side effects due to cross-inhibition of anti-target proteases. Successful examples of this strategy are represented by SB-3CT[10], a selective MMP-2 and MMP-9 inhibitor able to reduce prostate cancer metastasis to the bone[11] and T-cell lymphoma metastasis to the liver[12] in animal models, and *cis*-ACCP[13] a MMP-2 selective inhibitor with antimetastatic activity. A peculiar case is represented by NSC405020, an allosteric selective inhibitor of MMP-14 able to bind the hemopexin domain which significantly inhibited tumor growth in an animal model of breast cancer[14].

In our previous papers,[15,16] we described the synthesis and biological evaluation of *N*-isopropoxy-*N*-biphenylsulfonylaminobutyl hydroxamic acids as selective inhibitors of MMP-2 and MMP-14 for cancer therapy. In particular, compound **1** (ARP101, Figure 1) was found to be a potent

antiangiogenic agent, being able to block human umbilical vein endothelial cells (HUVEC) chemoinvasion at micromolar concentrations. Moreover the same compound, tested on the human glioma U87MG cell line, was shown to reduce cell invasion by 48% at nanomolar concentrations[17].

In the present paper, we report our optimization effort to identify novel *N*-isopropoxy-arylsulfonamide hydroxamates with improved inhibitory activity toward MMP-2, MMP-9 and MMP-14 with respect to **1**. Our starting hypothesis was that a simultaneous inhibition of all three MMPs involved in tumor-induced angiogenesis could have an increased effect against angiogenesis able to block tumor growth. A small series of new ethylamido α-substituted hydroxamates, **2a-g** and **3** (Figure 1), was designed and synthesized. These compounds were tested *in vitro* on recombinant MMPs, and the most promising derivatives were tested in the chemoinvasion assay, in order to verify the capability of endothelial cells to invade and digest a reconstituted basement membrane (matrigel). Finally, the *in vivo* antiangiogenic activity of **3** was determined using the matrigel sponge assay in mice.

FIGURE 1 HERE

2. Results.

Design of novel MMPs inhibitors. As already seen[18] the *N*-*O*-isopropyl substituent (P2' group, Figure 1) was important in order to achieve selectivity over MMP-1, while still maintaining activity against MMP-2. For this reason we chose to maintain the *N*-*O*-isopropyl group in the new series of sulfonamido derivatives. Moreover, the isopropyl substituent in the α position relative to the hydroxamate (P1 group) present in **1** was replaced with several *N*-ethylamido groups because changes at this level in similar arylsulfonamidic scaffolds had already given an improved activity against the target enzyme, ADAM-17, in previous studies[19]. In our hypothesis, the proper P1' substituent together with the *N*-*O*-isopropyl group should be able to direct the selectivity of the new compounds towards the target enzymes, while the presence of P1 substituents of variable size

should modulate their potency exploiting small changes in the S1 pocket between the different MMPs.

Chemistry. Optically active hydroxamates **2a-g** (Scheme 1) were prepared starting from the (*S*)-α-hydroxy-*tert*-butyl-ester **7**, which was synthesized as previously described.[15] A Mitsunobu condensation of sulfonamide **4-6**[18,20] with the alcohol **7** in the presence of diisopropyl azodicarboxylate (DIAD) and triphenylphosphine gave the *tert*-butyl esters (*R*)-**8-10**. *Tert*-butyl esters **14a-g** were obtained by Pd-catalyzed hydrogenation of **8-10** followed by acylation with commercial acyl chlorides, using *N*,*N*-diisopropylethylamine (DIPEA) as base. Acid cleavage of esters **14a-g** yielded carboxylates **15a-g** which were finally converted to their corresponding hydroxamates **2a-g** by condensation with *O*-(*tert*-butyldimethylsilyl)hydroxylamine followed by acid hydrolysis with TFA.

SCHEME 1 HERE

Hydroxamic acid **3** was synthesized as reported in Scheme 2, starting from the previously described alcohol **16**[19a]. A Mitsunobu coupling of sulfonamide **5** with the alcohol **16**, gave (*R*)-*tert*-butyl ester **17**. Acid cleavage of **17** yielded carboxylic acid **18** which was converted to its *O*-silylate derivative upon treatment with O-(*tert*-butyl-dimethylsilyl)hydroxylamine. Hydrolysis with trifluoroacetic acid of *tert*-butyl *O*-silylate provided hydroxamic acid **3**.

SCHEME 2 HERE

Biological activity on isolated enzymes. The new hydroxamic acids synthesized (**2a-g** and **3**) were tested *in vitro* on human recombinant MMPs by a fluorometric assay, which uses a fluorogenic peptide[21] as the substrate. Results are reported in Table 1, together with those already obtained for the previously described analogue **1**. The compounds were tested on MMP-2, -9 and -14, as

validated targets in cancer therapy, and MMP-1, considered as anti-target whose inhibition could be responsible for some side effects, such as musculoskeletal syndrome, clinically observed with the use of broad spectrum MMPIs.[22] Selectivity over MMP-3 was also evaluated because this enzyme was validated as potential anti-target in cancer therapy.[23] Finally, the activity against MMP-13 was also taken in consideration, given the recently reported role of this enzyme in promoting tumor angiogenesis.[24]

The replacement of the isopropyl substituent in the α position relative to the hydroxamate (P1 group) present in **1** with several *N*-ethylamido chains (compounds **2a-d**) caused a decrease of activity against MMP-14. This change did not affect activity against MMP-9 but derivative **2c** bearing an *N*-ethylacetoamido group in P1 resulted 2-fold more active than **1** on MMP-2 (Table 1), showing an IC_{50}=0.33 nM. Given these promising results, we chose to introduce a para-methoxy substituent on the biphenyl moiety (P1'group) present in **2c** in order to further increase activity and selectivity towards MMP-2 (known to be a deep-S1' pocket MMP). As expected, the para-methoxy-analogue of **2c**, compound **2e**, resulted about 6-fold more active than **1** on MMP-2, with an IC_{50}=0.13 nM. In a further attempt to expand the selectivity of action towards MMP-14, as our third target for the inhibition of tumor-induced angiogenesis controlled by MMPs, we decided to verify the effects of the introduction of a planar and lipophilic group in P1 on the scaffold of **2e** in place of its acetamido R_1 substituent. Therefore derivative **3**, bearing an *N*-ethylphthalimido substituent in P1, potentially able to give both hydrophobic π-π stacking interactions with aromatic residues and hydrogen bonds with the catalytic site of MMP-14, was synthesized. Actually, compound **3** gave the best inhibitory results on MMP-9 (IC_{50}=0.43 nM) and MMP-14 (IC_{50}=3.9 nM) still maintaining a sub-nanomolar activity on MMP-2 (IC_{50}=0.67 nM). The activity data on MMP-14 was noteworthy, given the lack of nanomolar small molecule MMP-14 inhibitors reported so far in literature. Moreover, compound **3** showed a 15-fold increase of activity towards MMP-9 and also an improved selectivity over MMP-1 and MMP-3 with respect to the reference compound **1**. On the contrary, the benzenesulfonamido derivative **2g** (R=H) showed a decrease of activity, in the

micromolar range, against all tested enzymes, probably due to the small size of its P1' group unable to properly fit in the S1' pocket of MMPs. This is a peculiarity of our *N*-*O*-isopropyl sulfonamido-based hydroxamates which have already shown different profiles of potency and selectivity[25] and associated lack of cell toxicity[20a,26] with respect to the other well known families of sulfonamide hydroxamates. In particular, the use of a short aromatic sulfonamido group is detrimental for this class of compounds (high micro-molar activity on all tested enzymes), while in all the other known classical sulfonamides (e.g. tertiary and secondary sulfonamides) this type of small substituent is often able to maintain nanomolar activities, without selectivity of action.[27]

The most promising compounds of this series, **2e** and **3**, were selected to be submitted to cell-based assays in order to prove their antiangiogenic activity, and we used **2g** as a negative control.

TABLE 1 HERE

Effect of MMP inhibitors on endothelial cell migration and invasion. The effects of **2e** and **3** on human umbilical vein endothelial cell (HUVEC) migration were assessed *in vitro*, and compared to those obtained using compound **2g**. The assay was performed using a modified Boyden chamber where fetal bovine serum (FBS) acted as a chemoattractant. Addition of 0.001 to 10 μM of compound **3** and **2e** resulted in an inhibition of endothelial cell migration, as compared to compound **2g** (Figure 2A-C). The strongest and significant (***$p<0.001$,* $p<0.05$) inhibitory effect on HUVEC migration was exerted by compound **3** in a dose dependent manner.

FIGURE 2 HERE

The effect of **3**, **2e** and **2g** on HUVEC invasion was evaluated using modified Boyden chambers[28] where 8 μm pore-size polycarbonate filters, pre-coated with a reconstituted basement membrane (matrigel, 10 mg/mL), were used as a barrier to invasion. Treatment with **2e** and **3** significantly

(***p<0.001, **p<0.01) reduced the FBS-induced HUVEC invasion as compared to **2g**, in a dose-dependent manner (Figure 3A-C). Interestingly, a significant inhibitory effect with **3** was observed already at the lower concentration (0.001 μM) (***p<0.001; Figure 3A).

FIGURE 3 HERE

Effect of MMP inhibitors on endothelial morphogenesis *in vitro*. When cultured in a 3-dimensional (3D) matrigel layer, HUVECs tend to organize into capillary-like-structures, mimicking *in vitro* the events that occur *in vivo* during angiogenesis. The addition of compound **3** significantly interfered with FBS-induced morphogenesis of HUVE cells in a dose dependent manner, restraining their ability to organize in a capillary-like network, as observed following 6 h of treatment and compared to compound **2e**, and **2g** (Figure 4A). Quantification of meshes, as a direct parameter to measure HUVEC network efficiency, showed a significantly decreased number of meshes (***p<0.001, *p<0.05) in cells treated with compound **3** as compared to **2e** and **2g** (Figure 4B).

FIGURE 4 HERE

Effect of MMP inhibitors on MMP-2 and MMP-9 levels by qPCR, western blot (WB) and gelatin zymography. The ability of compound **3** to interfere with MMP-2 transcript and protein levels was assessed by qPCR and confirmed by WB. Since HUVEC constitutively expressed only MMP-2, the cells were pre-stimulated under serum-free condition, with 30 nM PMA (Phorbol-12-myristate-13-acetate) to promote MMPs production. After PMA pre-treatment, low levels of MMP9 mRNA were detectable (data not shown). Both MMP-2 protein and mRNA were decreased following 24h of treatment with compound **3** (Figure 5A-B).

To investigate whether compounds **3** and **2e** were effectively able to inhibit MMP-2 and MMP-9 activity, gelatin zymography were performed on conditioned media (CM) obtained either from

untreated HUVECs, followed by exposition to increasing concentrations of **3**, **2e** and **2g** during the zymography, or conditioned media from HUVE cells exposed to the compounds **3** and **2g**. As shown in Figure 5C-D, both compound **3** and **2e** reduced MMP-2 and MMP-9 gelatinase activity in a dose-dependent manner, as compared to **2g**. Compound **3** showed a strong inhibitory effect already at low concentrations. The inhibitory effect of compound **3** starts from 0.001 μM, while for compound **2e**, which exerted a less pronounced gelatinase activity, inhibition was active from 0.1 μM. Compound **2g** showed no effect on the MMPs activities. We therefore evaluated the ability of **3** to inhibit MMP-2 and MMP-9 activity directly treating HUVE cells, using **2g** as a negative control. Cells were treated with **3** and **2g** 10 μM for 24 hours, using the same protocol for WB analysis. As shown in figure 5E-F-G only compound **3** significantly (**$p<0.01$) affected MMP release and production.

FIGURE 5 HERE

Effects of compound 3 on endothelial cell viability and induction of apoptosis. We explored the possibility that compound **3**, the most promising compound of this series, could exert non-selective toxicity or induce endothelial cell death. We analyzed proliferation by MTT (3-[4,5-dimethylthiazol-2-yl]-2,5 diphenyl tetrazolium bromide) assays and by staining with Annexin V and 7-amino-actinomycin D followed by flow cytometry analysis. No significant inhibition of endothelial cell growth was observed at different doses of compound **3** (Figure 6). Hydrogen peroxide (200 μM) induced apoptosis in approximately 20% of the cells (both Annexin V and 7-amino-actinomycin D positive; Figure 7). Cells treated with the inhibitor, even at highest concentrations, showed a high percentage (about 85%) of viable endothelial cells and no apoptosis (Figure 7). These data suggest that compound **3** does not exert toxicity or induce apoptosis in endothelial cells.

FIGURE 6 HERE

FIGURE 7 HERE

Effects of compound 3 on angiogenesis in vivo. We used the matrigel sponge assay model[29] as a rapid and quantitative system for measuring the *in vivo* the anti-angiogenic activity of compound **3**. Subcutaneous injection of matrigel produces a three-dimensional pellet that, when associated to angiogenic factors, becomes rapidly vascularized. VEGF, TNF-α, and heparin were used as angiogenic/inflammatory stimuli mixed with the matrigel, inducing an intense angiogenic reaction, as indicated indirectly by hemoglobin content. Addition of increasing concentrations of **3** to this mixture inhibited the *in vivo* angiogenic response (Figure 8A) decreasing hemoglobin content. To more precisely quantify the effects of compound **3** on angiogenesis, we quantified the number of endothelial cells in the pellets (identified as $CD45^-/CD31^+$ cells) by flow cytometry. The plugs excised from mice treated with compound **3** at 0.1-1-10 μM, both by adding the compound in the plugs and by IP injection (starting at day 0 of matrigel injection), showed significantly ($*p<0.05$) decreased number of $CD45^-/CD31^+$ cells in a dose dependent manner, as compared with VTH alone (Figure 8 B).

FIGURE 8 HERE

X-ray Crystallography and Molecular Modeling. To get an insight into the binding mode of compound **3** into the MMP-9 active site, X-ray crystallography studies were performed in comparison with the reference compound **1**.

The structures of three polymorphs of MMP-9 with **1** have been analyzed (Figure 9A). The trigonal crystal form (PDB code 4XCT) has not been reported before. The structure has been solved at 1.3 Å resolution, with a good refinement statistic (Table 1S, Supp. Information). The other crystal forms

with two molecules in the MMP-9 asymmetric unit have anisotropy problems not reported for other inhibitor complexes. Despite refinement problems, the three polymorphs show that the binding of **1** is well defined, except variability in the propyl and oxypropyl moieties (Figure 9B). The structure of the MMP-9-**3** complex (PDB code 4WZV) was determined in the monoclinic space group $P2_1$ at 1.65 Å resolution, with similar cell parameters as one of the structures determined for **1**. The refinement statistics are reported in Table 1S. The ligand is positioned in strong electron density (Figure 9C). The binding in the S1' pocket for the two ligands is identical and the two biphenyl rings overlap. Excluding the oxypropyl which in the MMP9 catalytic site, for **1** adopts a different orientation from that for **3**, there is also significant variation in the positioning of the sulfur oxygens between **1** and **3** (Figure 9D). The interaction that the sulfonamide oxygen makes for **1** with the protein backbone are at 2.90, 3.43 and 3.11 Å from the amide of Leu 188 and the carbonyl and amide of Ala 189, while the distances improve for **3** to 2.75, 3.4 and 3.13, respectively. Only a single additional direct hydrogen bond (2.97 Å) is observed between one of the phthaloyl carboxyl of **3** and the amide nitrogen of Ala 191 that in the **1** complex is made with a water molecule. The second phthaloyl carboxyl of **3** participates in promoting MMP-9 homodimerization, through an interaction with Tyr 420 via a water molecule (Figure 9E). The more precise positioning of **3** is likely to contribute to its higher affinity for MMP-9.

FIGURE 9 HERE

Since compound **3** showed a high inhibition activity also against MMP-2 and MMP-14, its interactions and binding disposition into these two MMPs were evaluated by means of docking studies followed by molecular dynamic simulations. The docking results highlighted that the binding orientation of the ligand into both MMPs was almost identical to that observed into the MMP9-**3** X-ray structure. Then, with the aim of verifying the stability of the inhibitor−enzyme interactions, the MMP-2-, MMP-9-, and MMP-14-**3** complexes were subjected to 5 ns of molecular

dynamic simulations (Figure 10). The ligand binding disposition suggested by the crystallographic structure was very stable for all the three MMPs with an average RMSD of about 1.2 Å, and with the maintenance of the lipophilic interactions of the biphenyl moiety inside the S1' cavity and the hydrogen bonds of the sulfonamide portion with the nitrogen backbone of L199 and A200 (MMP-9 residue number). Differently from that observed from the MMP9-**3** X-ray structure, the phthalimidic scaffold did not show H-bonds but in all three complexes showed a highly stable π-π interaction with the catalytic H243, that should be responsible for the high activity of this compound.

FIGURE 10 HERE

3. Discussion and Conclusions.

In this study, a new series of *N*-*O*-isopropyl sulfonamido-based hydroxamates with improved inhibitory activity toward MMP-2, MMP-9 and MMP-14 with respect to the previously discovered compound **1** was designed and synthesized. Among these compounds, two promising derivatives, **2e** and **3**, were identified by fluorometric assays on isolated enzymes and were chosen to be submitted to cell-based assays on HUVECs in order to assess their antiangiogenic activity. **2e** was a nanomolar inhibitor of MMP-2 and MMP-9, while **3** was a sub-nanomolar inhibitor of MMP-2 and MMP-9 but also a nanomolar inhibitor of MMP-14 (IC_{50}= 3.9 nM) selective over MMP-1 and MMP-3. X-ray crystallographic and docking studies validated the importance of the *N*-ethylphthalimido group for a proper positioning of **3** in the catalytic site of MMP-9 and MMP-14. First, the ability of the two compounds to inhibit gelatinase activity was evaluated on HUVEC conditioned medium derived either from untreated cells, further subjected to MMPI exposition or on directly MMPI-treated cells, by gelatin zymography and their efficacy was verified in the nanomolar range. Then, these two compounds were tested in the chemoinvasion assay, an in vitro model of angiogenesis able to quantify the invasive potential of endothelial cells, and in a

chemotaxis assay, used to measure the effect of **2e** and **3** on HUVEC migration. Compound **2g** was used as negative control in all these biological assays to prove our starting hypothesis that a simultaneous inhibition of all three MMPs involved in tumor-induced angiogenesis could have an increased effect against angiogenesis. In fact **2g** is MMP-2 inhibitor unable to inhibit MMP-9 and MMP-14 in the nanomolar range. From this screening, compound **3** emerged as the most active one, being able to block angiogenesis *in vitro* already at nanomolar concentrations while **2g** resulted inactive in all assays at the concentrations used. Moreover, **3** confirmed its activity in the matrigel sponge model in mice, without exerting toxicity or inducing apoptosis in endothelial cells. Taken together, these results supported our starting hypothesis that the simultaneous inhibition of all three MMPs (MMP-2, -9 and -14), sparing the anti-targets MMP-1 and -3, can represent an effective way to increase the antiangiogenic potential of MMP inhibitors to be exploited for cancer therapy, alone or in combination with cytotoxic compounds. Further studies will be necessary to demonstrate the efficacy of compound **3** to block tumor growth in human cancer models.

4. Experimental section

Chemistry. Melting points were determined on a Kofler hotstage apparatus and are uncorrected. ^{1}H and ^{13}C NMR spectra were determined with a Varian Gemini 200 MHz spectrometer or a Bruker Avance III HD 400 MHz spectrometer. Chemical shifts (δ) are reported in parts per million downfield from tetramethylsilane and referenced from solvent references. Coupling constants *J* are reported in hertz; ^{13}C NMR spectra were fully decoupled. The following abbreviations are used: singlet (s), doublet (d), triplet (t), double-doublet (dd), broad (br) and multiplet (m). Chromatographic separations were performed on silica gel columns by flash column chromatography (Kieselgel 40, 0.040–0.063 mm; Merck) or using ISOLUTE Flash Si II cartridges (Biotage). Reactions were followed by thin-layer chromatography (TLC) on Merck aluminum silica gel (60 F254) sheets that were visualized under a UV lamp and hydroxamic acids were visualized with $FeCl_3$ aqueous solution. Evaporation was performed *in vacuo* (rotating evaporator). Sodium

sulfate was always used as the drying agent. Commercially available chemicals were purchased from Sigma-Aldrich. Combustion analyses on target compounds were performed by our Analytical Laboratory in Pisa. All compounds showed >95% purity. See the Supporting Information for compound purity analysis data for final compounds.

General procedure for the preparation of (*R*)-*tert*-butyl esters 8-10. Diisopropyl azodicarboxylate (DIAD) (1.28 mL, 6.52 mmol) was added dropwise to a solution containing (*S*)-*tert*-butyl 4-(benzyloxycarbonylamino)-2-hydroxybutanoate **7** (0.8 g, 2.61 mmol), the appropriate sulfonamide **4-6** (3.91 mmol) and triphenylphosphine (2.05 g, 7.83 mmol) in anhydrous THF (45 mL) under nitrogen atmosphere at 0 ºC. The resulting solution was stirred for 5h at rt and evaporated under reduced pressure to afford a crude product, which was purified by flash chromatography on silica gel.

(*R*)-*tert*-Butyl 8-(biphenyl-4-ylsulfonyl)-10-methyl-3-oxo-1-phenyl-2,9-dioxa-4,8-diazaundecane-7-carboxylate (8). The title compound was prepared from *N*-isopropoxy-sulfonamide **4** following the general procedure. The crude was purified by flash chromatography on silica gel (*n*-hexane/EtOAc 5:1) to give a yellow oil (79% yield). ^{1}H-NMR ($CDCl_3$) δ**:** 1.22-1.25 (m, 15H); 2.04 (m, 2H); 3.22-3.37 (m, 2H); 4.12 (dd, *J*= 7.14 Hz, *J*= 14.29 Hz, 1H); 4.43 (septet, *J*= 6.2 Hz, 1H); 5.08 (s, 2H); 7.34 (m, 5H); 7.42-7.53 (m, 3H); 7.55-7.61 (m, 2H); 7.7-7.74 (m, 2H); 7.94-7.98 (m, 2H).

(*R*)-*tert*-Butyl 8-(4'-methoxybiphenyl-4-ylsulfonyl)-10-methyl-3-oxo-1-phenyl-2,9-dioxa-4,8-diazaundecane-7-carboxylate (9). The title compound was prepared from *N*-isopropoxy-sulfonamide **5** following the general procedure. The crude was purified by flash chromatography on silica gel (*n*-hexane/EtOAc 5:2) to give a yellow oil (74% yield). ^{1}H-NMR ($CDCl_3$) δ**:** 1.21-1.32 (m, 15H); 1.90-2.10 (m, 2H); 3.10-3.50 (m, 2H); 3.86 (s, 3H); 4.06-4.16 (m, 1H); 4.43 (septet, *J*= 6.2 Hz, 1H); 5.08 (s, 2H); 6.97-7.02 (m, 2H); 7.34 (m, 5H); 7.51-7.56 (m, 2H); 7.65-7.70 (m, 2H); 7.90-7.94 (m, 2H).

(*R*)-*tert*-Butyl 8-(4-bromophenylsulfonyl)-10-methyl-3-oxo-1-phenyl-2,9-dioxa-4,8-diazaundecane-7-carboxylate (10). The title compound was prepared from *N*-isopropoxy-sulfonamide **6** following the general procedure. The crude was purified by flash chromatography on silica gel (*n*-hexane/EtOAc 8:3) to give a yellow oil (87% yield). ^{1}H-NMR ($CDCl_3$) δ: 1.19-1.30 (m, 15H); 1.90-2.10 (m, 2H); 3.10-3.50 (m, 2H); 4.01-4.12 (m, 1H); 4.43 (septet, *J*= 6.2 Hz, 1H); 5.10 (s, 2H); 7.36 (m, 5H); 7.64-7.68 (m, 2H); 7.73-7.77 (m, 2H).

General procedure for the preparation of (*R*)-*tert*-butyl esters 11-13. A solution of the appropriate Cbz-derivative **8-10** (1.27 mmol) in MeOH (80 mL) was stirred under hydrogen atmosphere in the presence of 10% Pd-C (0.20 g) and glacial acetic acid (80 mL) for 17 h at rt. The resulting mixture was filtered on celite and the filtrate was evaporated under reduced pressure to give the deprotected salt.

(*R*)-4-*tert*-Butoxy-3-(*N*-isopropoxybiphenyl-4-ylsulfonamido)-4-oxobutan-1-aminium acetate (11). The title compound was prepared from Cbz-derivative **8** following the general procedure. Brownish oil, 93% yield. ^{1}H-NMR ($CDCl_3$) δ: 1.10 (brs, 9H); 1.20 (t, *J*= 4.4Hz, 6H); 2.16-2.30 (m, 2H); 3.16 (m, 2H); 4.34-4.46 (m, 2H); 7.40-7.51 (m, 3H); 7.56-7.59 (m, 2H); 7.71-7.75 (m, 2H); 8.00-8.04 (m, 2H). ^{13}C-NMR ($CDCl_3$) δ: 21.15; 21.22; 27.72; 36.70; 62.97; 80.03; 82.49; 127.03; 127.45; 127.59; 127.76; 128.67; 129.14; 130.49; 133.60; 139.30; 146.89.

(*R*)-4-*tert*-Butoxy-3-(*N*-isopropoxy-4'-methoxybiphenyl-4-ylsulfonamido)-4-oxobutan-1-aminium acetate (12). The title compound was prepared from Cbz-derivative **9** following the general procedure. Brownish oil, 95% yield. ^{1}H-NMR ($CDCl_3$) δ: 1.15-1.27 (m, 15H); 2.04-2.10 (m, 2H); 3.06 (m, 2H); 3.86 (s, 3H); 4.27 (m, 1H); 4.41 (septet, *J*= 6.2 Hz, 1H); 6.98-7.02 (m, 2H); 7.52-7.56 (m, 2H); 7.68-7.72 (m, 2H); 7.95-7.99 (m, 2H).

(*R*)-4-*tert*-Butoxy-3-(*N*-isopropoxyphenylsulfonamido)-4-oxobutan-1-aminium acetate (13). The title compound was prepared from Cbz-derivative **10** following the general procedure. Brown foam, 87% yield. ^{1}H-NMR ($CDCl_3$) δ: 1.17-1.33 (m, 15H); 2.17-2.40 (m, 2H); 3.22 (m, 2H); 4.33-4.50 (m, 1H); 5.04 (septet, *J*= 6.2 Hz, 1H); 7.53-7.66 (m, 3H); 7.96-8.00 (m, 2H).

General procedure for the preparation of (*R*)-*tert*-butyl esters 14a-g. A solution of the appropriate aminium acetate **11-13** (0.59 mmol) in dry DMF (6 mL) was treated with the appropriate acyl chloride (0.70 mmol) and *i*-Pr_2NEt (0.20 mL, 1.18 mmol). The reaction mixture was stirred at rt for 17h, then was diluted with AcOEt, washed with H_2O, dried over Na_2SO_4 and evaporated. The crude was purified by flash chromatography on silica gel.

(*R*)-*tert*-Butyl 4-benzamido-2-(*N*-isopropoxybiphenyl-4-ylsulfonamido)butanoate (14a). The title compound was prepared from aminium acetate **11** and benzoyl chloride following the general procedure. The crude was purified by flash chromatography on silica gel (*n*-hexane/EtOAc 2.5:1) to give **14a** as a yellow oil (34% yield). ^{1}H-NMR ($CDCl_3$) δ: 1.13 (brs, 9H); 1.23 (d, *J*= 5.1 Hz, 3H); 1.26 (d, *J*= 4.4Hz, 3H); 2.10-2.21 (m, 2H); 3.34-3.50 (m, 1H); 3.80-3.92 (m, 1H); 4.23 (t, *J*= 7.1 Hz, 1H); 4.45 (septet, 1H); 7.39-7.59 (m, 10H); 7.69-7.73 (m, 2H); 7.93-7.98 (m, 2H).

(*R*)-*tert*-Butyl 4-methanesulfonamido-2-(*N*-isopropoxybiphenyl-4-ylsulfonamido)butanoate (14b). A solution of **11** (0.30 g, 0.60 mmol) in dry THF (3 mL) was treated with methanesulfonyl chloride (0.05 mL, 0.60 mmol) and *N*-methylmorpholine (0.13 mL, 1.2 mmol). The reaction mixture was stirred at rt overnight, then was diluted with AcOEt, washed with H_2O, dried over Na_2SO_4 and evaporated. The crude was purified by flash chromatography (*n*-hexane/AcOEt = 3:2), to give **14b** (100 mg, 32 % yield) as a yellow oil. ^{1}H-NMR ($CDCl_3$) δ: 1.14 (brs, 9H); 1.20-1.26 (m, 6H); 2.04 (brs, 2H); 2.95 (s, 3H); 3.29 (brs, 2H); 4.25 (t, *J*= 7.1Hz, 1H); 4.42 (septet, 1H); 7.43-7.54 (m, 3H); 7.58-7.62 (m, 2H); 7.74-7.78 (m, 2H); 7.96-8.00 (m, 2H).

(*R*)-*tert*-Butyl 4-acetamido-2-(*N*-isopropoxybiphenyl-4-ylsulfonamido)butanoate (14c). The title compound was prepared from aminium acetate **11** and acetyl chloride following the general procedure. The crude was purified by flash chromatography on silica gel (*n*-hexane/EtOAc 1:1) to give **14c** as a yellow oil (22% yield). ^{1}H-NMR ($CDCl_3$) δ**:** 1.19-1.24 (m, 15H); 1.90-2.01 (m, 5H); 3.13-3.23 (m, 1H); 3.53 (m, 1H); 4.12 (m, 1H); 4.40 (septet, 1H); 6.11 (brs, 1H); 7.41-7.52 (m, 3H); 7.57-7.61 (m, 2H); 7.72-7.76 (m, 2H); 7.94-7.98 (m, 2H). ^{13}C-NMR ($CDCl_3$) δ: 21.17; 23.48;

27.76; 36.17; 63.59; 79.80; 82.25; 127.39; 127.52; 128.72; 129.16; 130.14; 133.80; 139.19; 146.84; 170.22.

(*R*)-*tert*-Butyl 2-(*N*-isopropoxybiphenyl-4-ylsulfonamido)-4-(2-phenylacetamido)butanoate (14d). The title compound was prepared from aminium acetate **11** and 2-phenylacetyl chloride following the general procedure. The crude was purified by flash chromatography on silica gel (*n*-hexane/EtOAc 2:1) to give **14d** as a yellow oil (20% yield). ^{1}H-NMR ($CDCl_3$) δ: 1.10-1.22 (m, 15H); 1.81-2.05 (m, 2H); 3.00-3.21 (m, 1H); 3.50-3.60 (m, 3H); 3.96 (t, *J*= 7.5Hz, 1H); 4.38 (septet, 1H); 7.28-7.37 (m, 5H); 7.43-7.54 (m, 3H); 7.57-7.62 (m, 2H); 7.68-7.73 (m, 2H); 7.80-7.84 (m, 2H).

(*R*)-*tert*-Butyl 4-acetamido-2-(*N*-isopropoxy-4'-methoxybiphenyl-4-ylsulfonamido)butanoate (14e). The title compound was prepared from aminium acetate **12** and acetyl chloride following the general procedure. The crude was purified by flash chromatography on silica gel (*n*-hexane/EtOAc 2:3) to give **14e** as a yellow oil (42% yield). ^{1}H-NMR ($CDCl_3$) δ: 1.19-1.25 (m, 15H); 1.90-2.04 (m, 5H); 3.13-3.50 (m, 2H); 3.87 (s, 3H); 4.12 (m, 1H); 4.41 (septet, 1H); 6.99-7.03 (m, 2H); 7.53-7.57 (m, 2H); 7.69-7.73 (m, 2H); 7.91-7.95 (m, 2H).

(*R*)-*tert*-Butyl 2-(*N*-isopropoxy-4'-methoxybiphenyl-4-ylsulfonamido)-4-(2-phenylacetamido)butanoate (14f). The title compound was prepared from aminium acetate **12** and 2-phenylacetyl chloride following the general procedure. The crude was purified by flash chromatography on silica gel (*n*-hexane/EtOAc 3:2) to give **14f** as a yellow oil (24% yield). ^{1}H-NMR ($CDCl_3$) δ: 1.16-1.25 (m, 15H); 1.90-2.05 (m, 2H); 3.12 (m, 2H); 3.57 (s, 2H); 3.87 (s, 3H); 3.94 (t, *J*= 7.5Hz, 1H); 4.37 (septet, 1H); 6.98-7.04 (m, 2H); 7.31-7.37 (m, 5H); 7.52-7.57 (m, 2H); 7.64-7.68 (m, 2H); 7.77-7.81 (m, 2H).

(*R*)-*tert*-Butyl 4-acetamido-2-(*N*-isopropoxyphenylsulfonamido)butanoate (14g). The title compound was prepared from aminium acetate **13** and acetyl chloride following the general procedure. The crude was purified by flash chromatography on silica gel (*n*-hexane/EtOAc 3:1) to

give **14g** as a yellow oil (55% yield). ^{1}H-NMR ($CDCl_3$) δ**:** 1.16-1.23 (m, 15H); 1.94 (s, 3H); 3.10-3.50 (m, 2H); 4.08 (m, 1H); 4.36 (septet, 1H); 7.49-7.69 (m, 3H); 7.87-7.92 (m, 2H).

General procedure for the preparation of (*R*)-carboxylic acids 15a-g. Trifluoroacetic acid (0.9 mL, 57.00 mmol) was added dropwise to a stirred solution of the appropriate *tert*-butyl ester **14a-g** (0.21 mmol) in freshly distilled CH_2Cl_2 (1.0 mL), cooled to 0°C. The solution was stirred for 5 h at 0°C and the solvent was removed in vacuo to give a crude that was purified by trituration with Et_2O/*n*-hexane.

(*R*)-4-Benzamido-2-(*N*-isopropoxybiphenyl-4-ylsulfonamido)butanoic acid (15a). The title compound was prepared from *tert*-butyl ester **14a** following the general procedure. Yellow oil, 99% yield. ^{1}H-NMR ($CDCl_3$) δ: 1.20 (t, *J*= 5.1 Hz, 6H); 1.80-2.28 (m, 2H); 3.40-3.55 (m, 1H); 3.60-3.82 (m, 1H); 4.30-4.50 (m, 2H); 6.56 (brs, 1H); 7.43-7.58 (m, 10H); 7.66-7.69 (m, 2H); 7.91-7.94 (m, 2H).

(*R*)-4-Methanesulfonamido-2-(*N*-isopropoxybiphenyl-4-ylsulfonamido)butanoic acid (15b). The title compound was prepared from *tert*-butyl ester **14b** following the general procedure. White solid, 79% yield. ^{1}H-NMR ($CDCl_3$) δ: 1.22 (d, *J*= 6.2 Hz, 6H); 2.06-2.17 (m, 2H); 2.91 (s, 3H); 3.21 (brs, 2H); 4.34-4.44 (m, 2H); 7.42-7.53 (m, 3H); 7.61-7.66 (m, 2H); 7.74-7.78 (m, 2H); 7.95-7.99 (m, 2H).

(*R*)-4-Acetamido-2-(*N*-isopropoxybiphenyl-4-ylsulfonamido)butanoic acid (15c). The title compound was prepared from *tert*-butyl ester **14c** following the general procedure. White solid, 80% yield. ^{1}H-NMR ($CDCl_3$) δ: 1.16 (d, *J*= 2.01 Hz, 3H); 1.19 (d, *J*= 2.01 Hz, 3H); 1.92-2.10 (m, 5H); 3.15-3.60 (m, 2H); 4.20-4.39 (m, 2H); 6.73 (brs, 1H); 7.42-7.52 (m, 3H); 7.59-7.63 (m, 2H); 7.73-7.77 (m, 2H); 7.93-7.97 (m, 2H); 10.24 (brs, 1H).

(*R*)-2-(*N*-isopropoxybiphenyl-4-ylsulfonamido)-4-(2-phenylacetamido)butanoic acid (15d). The title compound was prepared from *tert*-butyl ester **14d** following the general procedure. White solid, 70% yield. ^{1}H-NMR ($CDCl_3$) δ**:** 1.14 (d, *J*= 3.4 Hz, 3H); 1.17 (d, *J*= 3.4 Hz, 3H); 1.93-2.10 (m, 2H); 3.14 (m, 1H); 3.47 (m, 1H); 3.61 (s, 2H); 4.13 (t, *J*= 7.3 Hz, 1H); 4.33 (septet, 1H); 5.32

(brs, 1H); 6.14 (brs, 1H); 7.22-7.26 (m, 1H); 7.30-7.37 (m, 4H); 7.42-7.53 (m, 3H); 7.58-7.63 (m, 2H); 7.67-7.73 (m, 2H); 7.82-7.86 (m, 2H).

(*R*)-4-Acetamido-2-(*N*-isopropoxy-4'-methoxybiphenyl-4-ylsulfonamido)butanoic acid (15e). The title compound was prepared from *tert*-butyl ester **14e** following the general procedure. White solid, 67% yield. ^{1}H-NMR ($CDCl_3$) δ**:** 1.15-1.22 (m, 6H); 1.88-2.05 (m, 5H); 3.19-3.35 (m, 2H); 3.84 (s, 3H); 4.24 (t, 1H); 4.37 (septet, 1H); 6.30 (brs, 1H); 6.96-7.00 (m, 2H); 7.53-7.58 (m, 2H); 7.67-7.71 (m, 2H); 7.89-7.94 (m, 2H).

(*R*)-2-(*N*-isopropoxy-4'-methoxybiphenyl-4-ylsulfonamido)-4-(2-phenylacetamido)butanoic acid (15f). The title compound was prepared from *tert*-butyl ester **14f** following the general procedure. White solid, 70% yield. ^{1}H-NMR ($CDCl_3$) δ: 1.15 (d, *J*= 1.8 Hz, 3H); 1.18 (d, *J*= 1.8Hz, 3H); 1.93-2.10 (m, 2H); 3.10 (m, 2H); 3.56 (s, 2H); 3.86 (s, 3H); 4.15 (m, 1H); 4.37 (septet, 1H); 6.98-7.02 (m, 2H); 7.30-7.39 (m, 5H); 7.54-7.58 (m, 2H); 7.63-7.67 (m, 2H); 7.80-7.84 (m, 2H).

(*R*)-4-Acetamido-2-(*N*-isopropoxyphenylsulfonamido)butanoic acid (15g). The title compound was prepared from *tert*-butyl ester **14g** following the general procedure. White solid, 94% yield. ^{1}H-NMR ($CDCl_3$) δ**:** 1.18 (d, *J*= 2.01 Hz, 3H); 1.21 (d, *J*= 2.01 Hz, 3H); 1.63-1.80 (m, 2H); 1.97 (s, 3H); 3.15-3.50 (m, 2H); 4.24 (m, 1H); 4.37 (m, 1H); 6.05 (brs, 1H); 7.52-7.72 (m, 3H); 7.90-7.94 (m, 2H).

General procedure for the preparation of (*R*)-hydroxamic acids 2a-g. 1-[3-(Dimethylamino)propyl]-3-ethyl carbodiimide hydrochloride (EDC) was added portionwise (25 mg, 0.13 mmol) to a stirred and cooled solution (0 °C) of the appropriate carboxylic acid **15a-g** (0.087 mmol) and *O*-(*tert*-butyldimethylsilyl)hydroxylamine (12.8 mg, 0.087 mmol) in dry CH_2Cl_2 (2.2 mL). After stirring at room temperature overnight, the mixture was washed with water and the organic phase was dried and evaporated in vacuo.

Silyl precursors (0.05 mmol) were then dissolved in dry CH_2Cl_2 (0.4 mL) and TFA (0.22 mL, 2.8 mmol) was added dropwise at 0 °C. After 5 h of stirring, TFA was evaporated. The crude products were purified by trituration with *n*-hexane/Et_2O to give the desired hydroxamates **2a-g**.

(*R*)-*N*-(4-(Hydroxyamino)-3-(*N*-isopropoxybiphenyl-4-ylsulfonamido)-4-oxobutyl)benzamide (2a). The title compound was prepared from carboxylic acid **15a** following the general procedure. White solid, 60% yield. Mp: 125-127 °C; ^{1}H-NMR ($CDCl_3$) δ**:** 1.24 (t, *J*= 6.5Hz, 6H); 1.44-1.69 (m, 1H); 2.05-2.21 (m, 1H); 3.10-3.50 (m, 2H); 4.20-4.50 (m, 2H); 7.10 (brs, 1H); 7.30-7.55 (m, 10H); 7.59-7.63 (m, 2H); 7.86-7.90 (m, 2H). ^{13}C-NMR ($CDCl_3$) δ: 21.10; 27.21; 36.80; 60.90; 80.50; 127.40; 127.65; 128.89; 129.04; 129.14; 129.50; 129.87; 129.96; 132.61; 134.45; 138.80; 146.90; 167.50; 168.80.

(*R*)-4-Methanesulfonamido-*N*-hydroxy-2-(N-isopropoxybiphenyl-4-ylsulfonamido)butanamide (2b). The title compound was prepared from carboxylic acid **15b** following the general procedure. White solid, 60% yield. ^{1}H-NMR ($CDCl_3$) δ: 1.24 (t, *J*= 6.4Hz, 6H); 2.01-2.18 (m, 2H); 2.88 (s, 3H); 3.00-3.20 (m, 2H); 4.40-4.48 (m, 2H); 4.88 (brs, 1H); 7.42-7.53 (m, 3H); 7.62-7.66 (m, 2H); 7.78-7.83 (m, 2H); 7.95-7.99 (m, 2H). ^{13}C-NMR ($CDCl_3$) δ: 21.18; 27.15; 40.03; 40.25; 60.02; 80.64; 127.46; 127.92; 128.86; 129.13; 129.91; 130.06; 132.40; 138.82; 147.40; 167.35.

(*R*)-4-Acetamido-*N*-hydroxy-2-(*N*-isopropoxybiphenyl-4-ylsulfonamido)butanamide (2c). The title compound was prepared from carboxylic acid **15c** following the general procedure. Yellow oil, 70% yield. ^{1}H-NMR ($CDCl_3$) δ: 1.23 (d, *J*= 6.7 Hz, 6H); 1.90-2.08 (m, 5H); 3.04-3.35 (m, 2H); 4.22 (m, 1H); 4.40 (septet, 1H); 6.73 (brs, 1H); 7.42-7.52 (m, 3H); 7.59-7.63 (m, 2H); 7.76-7.80 (m, 2H); 7.92-7.96 (m, 2H). ^{13}C-NMR ($CDCl_3$) δ: 21.06; 23.18; 27.02; 36.89; 60.05; 80.72; 128.13; 129.36; 129.70; 130.57; 133.29; 139.74; 147.82; 166.70; 171.80.

(*R*)-*N*-Hydroxy-2-(*N*-isopropoxybiphenyl-4-ylsulfonamido)-4-(2-phenylacetamido)butanamide (2d). The title compound was prepared from carboxylic acid **15d** following the general procedure. White solid, 68% yield. Mp= 65-68 °C; ^{1}H-NMR ($CDCl_3$) δ: 1.18-1.32 (m, 6H); 1.83-2.22 (m, 2H); 3.10-3.28 (m, 2H); 3.48 (s, 2H); 4.11 (m, 1H); 4.39 (septet, 1H); 6.23 (brs, 1H); 7.16-7.36 (m, 5H); 7.43-7.47 (m, 3H); 7.57-7.61 (m, 2H); 7.67-7.72 (m, 2H); 7.86-7.90 (m, 2H). ^{13}C-NMR ($CDCl_3$) δ:

21.08; 27.05; 36.72; 43.39; 61.03; 80.04; 127.41; 127.67; 128.86; 129.04; 129.12; 129.48; 129.86; 129.98; 132.63; 134.46; 138.82; 147.24; 167.20; 172.38.

(*R*)-4-Acetamido-*N*-hydroxy-2-(*N*-isopropoxy-4'-methoxybiphenyl-4-ylsulfonamido)butanamide (2e). The title compound was prepared from carboxylic acid **15e** following the general procedure. White solid, 80% yield. Mp= 83-85 °C; ^{1}H-NMR ($CDCl_3$) δ: 1.20-1.26 (m, 6H); 1.94-2.04 (m, 5H); 3.02-3.40 (m, 2H); 3.86 (s, 3H); 4.22 (m, 1H); 4.45 (septet, 1H); 6.09 (brs, 1H); 6.98-7.02 (m, 2H); 7.55-7.59 (m, 2H); 7.71-7.75 (m, 2H); 7.89-7.94 (m, 2H). ^{13}C-NMR ($CDCl_3$) δ: 21.12; 27.20; 37.16; 55.41; 60.86; 80.42; 114.59; 127.03; 128.58; 129.84; 129.99; 131.08; 131.66; 146.80; 160.38; 167.72; 172.94.

(*R*)-*N*-Hydroxy-2-(*N*-isopropoxy-4'-methoxybiphenyl-4-ylsulfonamido)-4-(2-phenylacetamido)butanamide (2f). The title compound was prepared from carboxylic acid **15f** following the general procedure. White solid, 77% yield. Mp= 78-80 °C; ^{1}H-NMR ($CDCl_3$) δ: 1.19-1.22 (m, 6H); 1.94-1.98 (m, 2H); 3.00-3.20 (m, 2H); 3.51 (s, 2H); 3.86 (s, 3H); 4.10-4.16 (m, 1H); 4.41 (septet, 1H); 5.89 (brs, 1H); 6.97-7.01 (m, 2H); 7.21-7.32 (m, 5H); 7.53-7.57 (m, 2H); 7.65-7.69 (m, 2H); 7.83-7.87 (m, 2H). ^{13}C-NMR ($CDCl_3$) δ: 21.14; 26.90; 36.94; 43.28; 55.43; 60.83; 80.45; 114.59; 127.04; 127.53; 128.59; 129.11; 129.55; 129.85; 129.99; 131.08; 131.78; 134.18; 146.85; 160.41; 167.62; 172.84.

(*R*)-4-Acetamido-*N*-hydroxy-2-(*N*-isopropoxyphenylsulfonamido)butanamide (2g). The title compound was prepared from carboxylic acid **15g** following the general procedure. White semisolid, 65% yield. ^{1}H-NMR ($CDCl_3$) δ: 1.24 (d, *J*= 6.4 Hz, 6H); 1.70-1.85 (m, 2H); 1.95 (s, 3H); 3.01-3.18 (m, 2H); 4.10-4.20 (m, 1H); 4.43 (m, 1H); 6.00 (brs, 1H); 7.55-7.74 (m, 3H); 7.88-7.92 (m, 2H). ^{13}C-NMR ($CDCl_3$) δ: 21.09; 23.12; 26.90; 37.16; 60.02; 80.60; 127.03; 129.84; 131.80; 147.20; 164.70; 170.91.

(*R*)-*tert*-Butyl 4-(1,3-dioxoisoindolin-2-yl)-2-(*N*-isopropoxy-4'-methoxybiphenyl-4-ylsulfonamido)butanoate (17). Diisopropyl azodicarboxylate (DIAD) (0.4 mL, 2.0 mmol) was added dropwise to a solution containing (*S*)-*tert*-Butyl 4-(1,3-dioxoisoindolin-2-yl)-2-

hydroxybutanoate **16** (250 mg, 0.82 mmol), sulfonamide **5** (400 mg, 1.24 mmol) and triphenylphosphine (645 mg, 2.46 mmol) in anhydrous THF (12 mL) under nitrogen atmosphere at 0 ºC. The resulting solution was stirred for 5h at rt and evaporated under reduced pressure to afford a crude product, which was purified by flash chromatography on silica gel (*n*-hexane/AcOEt = 2:1), to give the desired product as a pale yellow oil (217 mg, 43% yield). ^{1}H-NMR ($CDCl_3$) δ: 1.24-1.29 (m, 15H); 2.10-2.30 (m, 2H); 3.51-3.74 (m, 2H); 3.87 (s, 3H); 4.06-4.23 (m, 1H); 4.46 (septet, 1H); 6.98-7.03 (m, 2H); 7.52-7.88 (m, 10H).

(*R*)-4-(1,3-Dioxoisoindolin-2-yl)-2-(*N*-isopropoxy-4'-methoxybiphenyl-4-ylsulfonamido)butanoic acid (18). Trifluoroacetic acid (1.5 mL, 18.8 mmol) was added dropwise to a stirred solution of *tert*-butyl ester **17** (205 mg, 0.33 mmol) in freshly distilled CH_2Cl_2 (2.0 mL), cooled to 0°C. The solution was stirred for 5 h at 0 °C and the solvent was removed in vacuo to give a crude that was purified by trituration with Et_2O/*n*-hexane. White solid, 135 mg, 74% yield. Mp= 185-187 °C; ^{1}H-NMR ($CDCl_3$) δ: 1.21 (d, *J*= 6.2Hz, 3H); 1.27 (d, *J*= 6.2Hz, 3H); 2.10-2.28 (m, 2H); 3.61 (m, 2H); 3.87 (s, 3H); 4.33 (m, 1H); 4.46 (septet, 1H); 6.98-7.02 (m, 2H); 7.50-7.54 (m, 4H); 7.65-7.85 (m, 6H).

(*R*)-4-(1,3-Dioxoisoindolin-2-yl)-*N*-hydroxy-2-(*N*-isopropoxy-4'-methoxybiphenyl-4-ylsulfonamido)butanamide (3). 1-[3-(Dimethylamino)propyl]-3-ethyl carbodiimide hydrochloride (EDC) was added portionwise (65 mg, 0.34 mmol) to a stirred and cooled solution (0 °C) of carboxylic acid **18** (130 mg, 0.23 mmol) and *O*-(*tert*-butyldimethylsilyl)hydroxylamine (51 mg, 0.34 mmol) in dry CH_2Cl_2 (7.0 mL). After stirring at room temperature overnight, the mixture was washed with water and the organic phase was dried and evaporated in vacuo.

Silyl precursor (100 mg, 0.14 mmol) was then dissolved in dry CH_2Cl_2 (1.0 mL) and TFA (0.6 mL, 7.9 mmol) was added dropwise at 0 °C. After 5 h of stirring, TFA was evaporated. The crude product was purified by trituration with *n*-hexane/Et_2O to give the desired hydroxamate **3** as a white solid (61 mg, 77% yield). Mp= 75-76 °C; ^{1}H-NMR ($CDCl_3$) δ: 1.23 (d, *J*= 6.2Hz, 3H); 1.30 (d, *J*= 6.2Hz, 3H); 2.12-2.32 (m, 2H); 3.40-3.53 (m, 2H); 3.88 (s, 3H); 4.02-4.20 (m, 1H); 4.46 (septet, *J*=

6.2Hz, 1H); 6.98-7.02 (m, 2H); 7.29-7.39 (m, 2H); 7.42-7.46 (m, 2H); 7.63 (m, 4H); 7.72-7.76 (m, 2H). ^{13}C-NMR ($CDCl_3$) δ: 21.15; 26.80; 34.75; 55.44; 60.72; 80.08; 114.50; 123.29; 127.03; 128.63; 129.88; 131.32; 131.81; 132.01; 133.94; 134.23; 146.81; 160.30; 166.85; 168.23.

MMP inhibition assays. Recombinant human progelatinase A (pro-MMP-2), B (pro-MMP-9), and MMP-14 catalytic domain were a kind gift of Prof. Gillian Murphy (Department of Oncology, University of Cambridge, UK). Pro-MMP-1, pro-MMP-13 and pro-MMP-3 were purchased from Calbiochem. Proenzymes were activated immediately prior to use with *p*-aminophenylmercuric acetate (APMA 2 mM for 1 h at 37 °C for MMP-2, 1 mM for 1 h at 37 °C for MMP-9, 2 mM for 2 h at 37 °C for MMP-1, 1 mM for 35 min at 37 °C for MMP-13). Pro-MMP-3 was activated with trypsin (4.4 μg/mL) for 30 min at 37 °C followed by addition of soybean trypsin inhibitor (61.5 μg/mL). For assay measurements, the inhibitor stock solutions (DMSO, 10 mM) were further diluted in the fluorimetric assay buffer (FAB: Tris 50 mM, pH = 7.5, NaCl 150 mM, $CaCl_2$ 10 mM, Brij 35 0.05% and DMSO 1%). Activated enzyme (final concentration 0.5 nM for MMP-2, 1.3 nM for MMP-9, 1.0 nM for MMP-14cd, 2.0 nM for MMP-1, 0.66 nM for MMP-13 and 5 nM for MMP-3) and inhibitor solutions were incubated in the assay buffer for 4 h at 25 °C. After the addition of 200 μM solution of the fluorogenic substrate Mca-Lys-Pro-Leu-Gly-Leu-Dap(Dnp)-Ala-Arg-NH_2 (Bachem) in DMSO (final concentration 2 μM), the hydrolysis was monitored every 10 s for 20 min recording the increase in fluorescence (λ_{ex} = 325 nm, λ_{em} = 395 nm) using a Molecular Devices SpectraMax Gemini XS plate reader. The assays were performed in a total volume of 200 μL per well in 96-well microtitre plates (Corning, black, NBS). Control wells lack inhibitor. The MMP inhibition activity was expressed in relative fluorescent units (RFU). Percent of inhibition was calculated from control reactions without the inhibitor. IC_{50} was determined using the formula: $v_i/v_o = 1/(1 + [I]/ IC_{50})$, where v_i is the initial velocity of substrate cleavage in the presence of the inhibitor at concentration [I] and v_o is the initial velocity in the absence of the inhibitor. Results were analyzed using SoftMax Pro software[30] and GraFit software.[31]

Cell cultures

Human umbilical vein endothelial cells (HUVECs) were purchased from Promo Cell (Heidelberg, Germany) and grown on 1% gelatin-coated tissue culture plates in Medium 199 (Sigma Aldrich Milano), supplemented with 10% heat-inactivated fetal bovine serum (FBS) (Euroclone, Milano), 1% glutamine (Euroclone, Milano), fibroblast growth factors (1μg/100mL acid-fibroblast growth factor plus 1μg/ 100mL basic-fibroblast growth factor, PeproTech London UK), epidermal growth factor (1μg/100mL PeproTech London UK), heparin (10mg/100mL, Sigma Aldrich Milano) and hydrocortisone (0.1mg/100mL Sigma Aldrich Milano) at 37 °C in 5 % CO_2. Cells were used between the third and sixth passage *in vitro*.

$2x10^6$ cells were seeded in a six-well plate and after one day of attachment, cells were starved 6 h in serum-free medium with BSA 2%. Cells were then pre-treated for 3 h with 30 nM PMA, followed by exposition to compound **3** or **2g**. DMSO was used as vehicle in untreated cells. After 24 hours, conditioned media were collected for zymography and cells were processed both for RNA and proteins extraction.

Chemotaxis and chemoinvasion assays. Migration and invasion assays were performed using modified Boyden chambers[28]. Human endothelial cells (HUVEC) ($5x10^4$) were washed with PBS, resuspended in serum-free medium and placed in the upper compartment of the chamber, in presence/absence of different concentrations of inhibitors. Chemoattractant (10% FBS) or serum free medium were added in the lower compartment. Pore-size polycarbonate filters (8 μM) were pre-coated with collagen (50 μg/mL) or matrigel (1 mg/mL) and used as the interface between the two chambers compartments. Following 6 h (migration) or overnight (invasion) incubation, the filters were recovered, cells on the upper surface mechanically removed using a cotton swab; cells migrated or invaded to the lower filter surface fixed with absolute ethanol and stained with Vectashield mounting medium (Vector Laboratories, Burlingame, CA, USA). Cells were counted in a double-blind manner in eight consecutive fields each with a light microscope. All experiments were performed three times in duplicate. Statistical significance was determined by One way ANOVA using GraphPad Prism.

Matrigel morphogenesis assay. The *in vitro* morphogenesis assay was performed in presence of 10% FBS and different concentration of inhibitors. Briefly, a 24-microwell plate, pre-chilled at -20 °C, was carefully filled with 300 µL/well of liquid matrigel (10 mg/mL) at 4 °C with a pre-chilled pipette, avoiding bubbles. The matrigel was then polymerized for 1 h at 37 °C, and HUVEC ($50x10^4$ cells/well) were suspended in 1 mL of complete medium in the absence or presence of different concentrations of inhibitors and carefully layered on the top of the polymerized matrigel. After 6 h incubation on matrigel, the dimensional organization of the cells was examined under an inverted microscope (Zeiss, Oberkochen, Germany), equipped with CCD optics and a digital analysis system. The number of meshes where measured, as a direct parameter for HUVEC tubulogenic efficiency, using the Angiogenesis tool and ImageJ software.[32] Statistical significance was determined by Oneway ANOVA using GraphPad Prism.

Quantitative reverse trascription-PCR. Total RNA was extracted from cells using the RNeasy Protect Mini Kit (Qiagen, Hilden, Germany) according to the recommendation of the manufacturer and reverse transcribed as above with oligo dT primers in 20µL final volume. All primers for the genes tested were designed using primer3 software[33] with a Tm optimum of approximately 60 °C and a product length of 100-150nt. Real time PCR was performed on a LightCycler480 (Roche, Penzberg, Germany) using Light Cycler 480 SYBR Green I Master (Roche), 3 µL of cDNA (10x diluted), 3 pmol sense and anti-sense primers in a final reaction volume of 10 µL. After an initial denaturation step of 5 min during which the well factor was measured, 45 cycles of 10 s at 95 °C followed by 15 s at 60 °C and 15 s at 72 °C were performed. Fluorescence was measured during the annealing step in each cycle. After amplification melting curves with 80 steps of 15 s and 0.5 °C increase were performed to monitor amplicon identity. Expression data were normalized on the mean of the expression values for three housekeeping genes: cyclophilin A, 16 s rRNA (ribosomal RNA) and GUSB (β-glucuronidase). Relative expression values with standard errors and statistical comparisons (unpaired two-tailed t-test) were obtained using Qgene software.

Western Blot. HUVE cells were grown as indicated and collected by brief trypsinization. Total lysates were prepared using cell lysis buffer (Cell Signaling Technology, Beverly, MA). Protein concentrations were evaluated by the DC Protein Assay (Bio-Rad, Hercules, CA). Equal amounts of proteins for each sample were resolved on 10% sodium dodecyl sulfate–polyacrylamide gel electrophoresis and blotted onto polyvinylidene fluoride membranes (Amersham Biosciences, Otelfingen, CH). Following blocking with 5% non-fat milk powder (wt/vol) in Tris-buffered saline (10 mM Tris–HCl, pH 7.5, 100 mM NaCl, 0.1% Tween-20) for 1 h at room temperature, membranes were incubated with primary antibodies directed against the following human antigens: MMP-2, MMP-9 (all purchased from Cell Signaling Technology, Danvers, MA) and β-actin (Sigma Aldrich, Milan). The antibodies were diluted in 2% bovine serum albumin–Tris-buffered saline–0.1% Tween according to the manufacturer's instructions. The bound antibodies were visualized by horseradish-peroxidase- conjugated secondary antibodies and an enhanced chemiluminescence detection system from Amersham Biosciences (Pittsburg, PA).

Zymographic Analysis. The effects of compounds on gelatinases activity was determined by gel zymography either on MMPs derived from not-treated HUVEC media, further exposed to MMP inhibitors or by using CM directly derived from MMP-inhibitors treated HUVE cells. Without heating the samples, 20 μL of untreated HUVEC conditioned medium or an equal amounts of protein derived from treated HUVECs were loaded 10% polyacrylamide additioned of 0.1% gelatin, in presence of SDS. Following electrophoresis, the gels were incubated for 30 min at room temperature with gentle agitation in Renaturing Buffer (Invitrogen, Eugene, OR, USA). For gelatinase inhibition assays of not-treated HUVEC, the different inhibitors were added in the Developing Buffer (Invitrogen, Eugene, OR, USA) over night at 37 °C; the gel slab was cut into slices corresponding to the lanes and then put in different tanks containing the stated concentrations of inhibitors. For MMPI treated HUVEC, gels were directly incubated over night at 37 °C in Developing Buffer. Gels were then stained for 15 min with Coomassie Brillant Blue R-250 stain and then de-stained with 10% acetic acid and 30% methanol until sharp bands were visualized.

Band intensities were quantified by densitometric analysis using ImageJ software (National Institutes of Health).

MTT assay. Human umbilical vein endothelial cell viability was evaluated using the MTT assay. Cells (1000/well) were seeded into 96-multiwell plates in complete medium and, after complete adhesion, the medium was replaced with fresh medium with or without different concentrations of compound **3** (10 nM-10 μM). After different periods of incubation (24, 48, 72 and 96 h), plates were processed and absorbance read at 570 nm.

Assessment of apoptosis by Flow Cytometry. Human umbilical vein endothelial cells ($1x10^5$) were plated onto six-well plates and allowed to adhere overnight. The next day, cells were treated in the growth medium with increasing concentration of the inhibitor (10 nM- 10 μM). Growth medium alone (NT) and hydrogen peroxide (100- 200 μM) were used as controls. After overnight, cells were recovered, washed with PBS and transferred to test tubes. Cells were pelleted and resuspended in Annexin V-binding buffer (0.01 M HEPES (4-(2-hydroxyethyl)-1-piperazineethanesulfonic acid) pH 7.4; 0.14 M NaCl; 2.5 mM $CaCl_2$). Fluorescein isothiocyanate Annexin V and 7-amino-actinomycin D (BD Biosciences) were added to each test tube and incubated for 15 min at room temperature in the dark. Cells were then washed in PBS, supernatants discarded and resuspended in 400 mL of binding buffer. Samples were acquired by flow fluorocytometry using a FACSCanto (BD Biosciences) and analyzed using FACSDiva Software 6.1.2.

Matrigel sponge assay (in vivo angiogenesis). The assay was performed as already described[29]. VTH mixture (100 ng/mL VEGF-A, 2 ng/mL TNF-α, and 25 UI/mL heparin), either alone or in combination with compound **3** at 0.1-1-10 μM, was added to unpolymerized liquid matrigel at 4 °C and the mixture was brought to a final volume of 0.6 mL. The matrigel suspension was then slowly injected subcutaneously into the flanks of C57/BL6 male mice (Charles River, Calco [Lecco], Italy) with a cold syringe. At body temperature *in vivo*, the matrigel quickly polymerizes to form a solid gel. In some experiments the mice were also treated with 0.1-1-10 μM of compound **3** by intraperitoneal (i.p.) injection, at day 0. Groups of 8 mice were used for each treatment. Four days

after injection, the gels were recovered, weighted, minced and diluted in PBS to measure the hemoglobin content with a Drabkin reagent kit (Sigma, St Louis, MO, USA). Part of the pellets recovered were assessed for endothelial cell infiltrate quantification by multicolor flow cytometry. Briefly, pellets were digested for 1 h in 1 mg/mL Collagenase IV. The cell suspension obtained was stained with anti-murine mab as follows: APC-CD45, FITC-CD31, PerCP-CD3, finally analyzed by flow cytometry. Endothelial cells in the total cell suspension, gated on FSC/SSC-selected viable cells, were quantified as the % of $CD31^+$ cells, on $CD45^-CD3^-$ gated cells.

Statistical analysis. Results are showed as mean ± SEM. The significance of differences was evaluated with a two-tailed t-test or One way ANOVA test using Prism software (GraphPad Software for Science, Inc., San Diego, CA, USA).

Docking Calculations. The crystal structure of MMP-2 (PDB code 1QIB), MMP-9 (PDB code 4WZV), and MMP-14 (PDB code 3MA2) was taken from the Protein Data Bank.[34] After adding hydrogen atoms the three proteins were minimized using Amber 11 software[35] and parm03 force field at 300 K. The three proteins were placed in a rectangular parallelepiped water box, an explicit solvent model for water, TIP3P, was used and the complexes were solvated with a 10 Å water cap. Sodium ions were added as counter ions to neutralize the system. Two steps of minimization were then carried out; in the first stage, we kept the protein fixed with a position restraint of 500 kcal/mol•$Å^2$ and we solely minimized the positions of the water molecules. In the second stage, we minimized the entire system through 5000 steps of steepest descent followed by conjugate gradient (CG) until a convergence of 0.05 kcal/Å•mol. Automated docking was carried out by means of the AUTODOCK 4.0 program;[36] Autodock Tools[37] was used in order to identify the torsion angles in the ligand, add the solvent model and assign the Kollman atomic charges to the protein. The ligand charge was calculated using the Gasteiger method.

A grid spacing of 0.375 Å and a distance-dependent function of the dielectric constant were used for the energetic map calculations. Using the Lamarckian Genetic Algorithm, the docked compound was subjected to 100 runs of the Autodock search, using 500000 steps of energy evaluation and the

default values of the other parameters. Cluster analysis was performed on the results using an RMS tolerance of 2.0 Å and the best docked conformation was taken into account.

MD Simulations.

All simulations were performed using AMBER, version 11. MD simulations were carried out using the parm03 force field at 300 K. The complex was placed in a rectangular parallelepiped water box. An explicit solvent model for water, TIP3P, was used, and the complex was solvated with a 10 Å water cap. Sodium ions were added as counterions to neutralize the system. Prior to MD simulations, two steps of minimization were carried out using the same procedure described above. Particle mesh Ewald (PME) electrostatics and periodic boundary conditions were used in the simulation.[38] The MD trajectory was run using the minimized structure as the starting conformation. The time step of the simulations was 2.0 fs with a cutoff of 10 Å for the nonbonded interaction, and SHAKE was employed to keep all bonds involving hydrogen atoms rigid. Constant-volume periodic boundary MD was carried out for 500 ps, during which the temperature was raised from 0 to 300 K. Then 4.5 ns of constant pressure periodic boundary MD was carried out at 300 K using the Langevin thermostat to maintain constant the temperature of our system. All the α carbons of the protein were blocked with a harmonic force constant of 10 kcal/mol•Å^2. General Amber force field (GAFF) parameters were assigned to the ligand, while partial charges were calculated using the AM1-BCC method as implemented in the Antechamber suite of AMBER 11. The final structure of the complex was obtained as the average of the last 3.0 ns of MD minimized by the CG method until a convergence of 0.05 kcal/mol•Å^2. The average structure was obtained using the ptraj program implemented in AMBER 11.

Crystallization and Structure determination. The expression and purification of MMP-9 was carried out as previously described.[39] In brief, MMP-9 comprises residues Met109–Gly215 and Gln391–Gly444, without the additional fibronectin domains. Plasmids were propagated in the *Escherichia coli* strain XL1-Blue and the recombinant catalytic domains expressed in *E. coli* cells BL21 (DE3 star). The protein was refolded from inclusion bodies, and purified as previously

described. Acetohydroxamic acid (AHA) 120 mM was added to prevent self-degradation and MMP-9 concentrated to 337 μM. Detail for the final crystallization conditions used for growing crystals are given in Table 1S for both MMP-9 complexes. Prior to data collection at the Soleil synchrotron (St. Aubin, France) on beamline Proxima 1, crystals were transferred to an appropriate mixed cryoprotectant solution.[40] Data was reduced using XDS[41] and the script "xdsme". The crystal of the complex MMP-9●**3** belonged to the space group $P2_1$ and diffracted to 1.65 Å resolution (Table 1S). The structure was solved by rigid body refinement using REFMAC5[42] build using the monomer library sketcher from CCP4 program suite,[43] the model rebuilt with COOT[44] followed by cycles of REFMAC5 and phenix.refine.[45] Crystals for the MMP-9●**1** complex were grown in three different polymophs[39] but the first two attempts were unsatisfactory. Crystals in the space orthorhombic $P2_12_12$ with cell parameters a = 74.1 Å, b = 98.5 Å, c = 46.1 at 1.9 Å, resulted in a structure with R=26.8% and R-free 35.4% because of anisotropy. The related monoclinic enatiomorph, $P2_1$ with cell parameters a = 39.9 Å, b = 97.4 Å, c = 46.1, β=111.9° gave data to 1.98 Å with acceptable refinement statistics, R 19.6% and R-free 26.5%. The best diffraction was obtained with stimulated nucleation by streak seeding[46] in the trigonal space group because groups $P3_221$ with cell parameters $a = b$ = 39.6 c = 163.96 at 1.3 Å (Table 1S).

Accession codes. The crystal structure data for the MMP-9 in complex with **1** and **3** have been deposited at Protein Data Bank with accession codes 4XCT and 4WZV, respectively.

Acknowledgment. The authors are grateful to the French synchrotron SOLEIL for allocation of beam time and to Drs. Isabet and Legrande for assistance during data collection. This study was supported by fundings from the Italian Ministry of Education, University and Research (MIUR, PRIN 2010, 20109MXHMR_007, E. N. and S.N.), from the University of Pisa (Fondi di Ateneo 2013, rating 2014 to A. R. and E. N.) and from the Italian Association for Cancer Research (AIRC 10228 to A. A.).

Supporting Information Available: A table reporting the combustion analysis data of the final products, a table with statistics for MMP-9 data collection, processing and refinement (crystallographic data) and a Supplementary figure. This material is available free of charge via the Internet at http://pubs.acs.org.

Abbreviations used.

HUVEC, human umbilical vein endothelial cells; MMPI, MMP inhibitor; ECM, extracellular matrix; MSS, musculoskeletal syndrome; DIAD, diisopropyl azodicarboxylate; DIPEA, *N*,*N*-diisopropylethylamine; EDC, *N*-(3-Dimethylaminopropyl)-N′-ethylcarbodiimide hydrochloride; SAR, structure-activity relationship; FBS, foetal bovine serum; APMA, *p*-aminophenylmercuric acetate; FAB, fluorimetric assay buffer; RFU, relative fluorescent units; SD, standard deviation; AHA, acetohydroxamic acid.

References

(1) Stetler-Stevenson, W. G. Matrix metalloproteinases in angiogenesis: a moving target for therapeutic intervention. *J. Clin. Invest.* **1999**, *103*, 1237–1241.

(2) Correa de Sampaio, P.; Auslaender, D.; Krubasik, D.;, Failla, A. V.; Skepper, J. N.; Murphy, G.; English, W. R. A heterogeneous in vitro three dimensional model of tumour-stroma interactions regulating sprouting angiogenesis. *PLoS One.* **2012**, *7*, e30753.

(3) Rundhaug, J. E. Matrix metalloproteinases and angiogenesis. *J. Cell. Mol. Med.* **2005**, *9*, 267-285.

(4) Fang, J.; Shing, Y.; Wiederschain, D.; Yan, L.; Butterfield, C.; Jackson, G.; Harper, J.; Tamvakopoulos, G.; Moses, M. A. Matrix metalloproteinase-2 is required for the switch to the angiogenic phenotype in a tumor model. *Proc. Natl. Acad. Sci. U S A.* **2000**, *97*, 3884-3889.

(5) Deryugina, E. I.; Quigley, J. P. Matrix metalloproteinases and tumor metastasis. *Cancer Metastasis Rev*. **2006**, *25*, 9-34.

(6) Basile, J. R.; Holmbeck, K.; Bugge, T. H.; Gutkind, J. S. MT1-MMP controls tumor-induced angiogenesis through the release of semaphorin 4D. *J. Biol. Chem.* **2007**, *282*, 6899-6905.

(7) Sato, H.; Takino, T. Coordinate action of membrane-type matrix metalloproteinase-1 (MT1-MMP) and MMP-2 enhances pericellular proteolysis and invasion. *Cancer Sci*. **2010**, *101*, 843-847.

(8) Devy, L.; Huang, L.; Naa, L.; Yanamandra, N.; Pieters, H.; Frans, N.; Chang, E.; Tao, Q.; Vanhove, M.; Lejeune, A.; van Gool, R.; Sexton, D. J.; Kuang, G.; Rank, D.; Hogan, S.; Pazmany, C.; Ma, Y. L.; Schoonbroodt, S.; Nixon, A. E.; Ladner, R. C.; Hoet, R.; Henderikx, P.; Tenhoor, C.; Rabbani, S. A.; Valentino, M. L.; Wood, C. R.; Dransfield, D. T. Selective inhibition of matrix metalloproteinase-14 blocks tumor growth, invasion, and angiogenesis. *Cancer Res*. **2009**, *69*, 1517-1526.

(9) Coussens, L. M.; Fingleton, B.; Matrisian, L. M. Matrix metalloproteinase inhibitors and cancer: trials and tribulations. *Science* **2002**, *295*, 2387–2392.

(10) Brown, S.; Bernardo, M. M.; Li, Z. H.; Kotra, L. P.; Tanaka, Y.; Fridman, R.; Mobashery, S. Potent and selective mechanism-based inhibition of gelatinases. *J. Am. Chem. Soc.* **2000**, *122*, 6799−6800.

(11) Bonfil, R. D.; Sabbota, A.; Nabha, S.; Bernardo, M. M.; Dong, Z.; Meng, H.; Yamamoto, H.; Chinni, S. R.; Lim, I. T.; Chang, M.; Filetti, L. C.; Mobashery, S.; Cher, M. L.; Fridman, R. Inhibition of human prostate cancer growth, osteolysis and angiogenesis in a bone metastasis model by a novel mechanism-based selective gelatinase inhibitor. *Int. J. Cancer* **2006**, *118*, 2721–2726.

(12) Kruger, A.; Arlt, M. J. E.; Gerg, M.; Kopitz, C.; Bernardo, M. M.; Chang, M.; Mobashery, S.; Fridman, R. Antimetastatic activity of a novel mechanism-based gelatinase inhibitor. *Cancer Res.* **2005**, *65*, 3523–3526.

(13) Hoffman, A.; Qadri, B.; Frant, J.; Katz, Y.; Bhusare, S. R.; Breuer, E.; Hadar, R.; Reich, R. Carbamoylphosphonate matrix metalloproteinase inhibitors 6: cis-2-aminocyclohexylcarbamoylphosphonic acid, a novel orally active antimetastatic matrix

metalloproteinase-2 selective inhibitor--synthesis and pharmacodynamic and pharmacokinetic analysis. *J. Med. Chem.* **2008**, *51*, 1406-1414.

(14) Remacle, A. G.; Golubkov, V. S.; Shiryaev, S. A.; Dahl, R.; Stebbins, J. L.; Chernov, A. V.; Cheltsov, A. V.; Pellecchia, M.; Strongin, A. Y. Novel MT1-MMP small-molecule inhibitors based on insights into hemopexin domain function in tumor growth. *Cancer Res.* **2012**, *72*, 2339-2349.

(15) Rossello, A.; Nuti, E.; Carelli, P.; Orlandini, E.; Macchia, M.; Nencetti, S.; Zandomeneghi, M.; Balzano, F.; Uccello Barretta, G.; Albini, A.; Benelli, R.; Cercignani, G.; Murphy, G.; Balsamo, A. N-i-Propoxy-N-biphenylsulfonylaminobutylhydroxamic acids as potent and selective inhibitors of MMP-2 and MT1-MMP. *Bioorg. Med. Chem. Lett.* **2005**, *15*, 1321-1326.

(16) Tuccinardi, T.; Martinelli, A.; Nuti, E.; Carelli, P.; Balzano, F.; Uccello-Barretta, G.; Murphy, G.; Rossello, A. Amber force field implementation, molecular modelling study, synthesis and MMP-1/MMP-2 inhibition profile of (R)- and (S)-N-hydroxy-2-(N-isopropoxybiphenyl-4-ylsulfonamido)-3-methylbutanamides. *Bioorg. Med. Chem.* **2006**, *14*, 4260-4276.

(17) Gabelloni, P.; Da Pozzo, E.; Bendinelli, S.; Costa, B.; Nuti, E.; Casalini, F.; Orlandini, E.; Da Settimo, F.; Rossello, A.; Martini, C. Inhibition of metalloproteinases derived from tumours: new insights in the treatment of human glioblastoma. *Neuroscience*. **2010**, 168, 514-522.

(18) Nuti, E.; Casalini, F.; Avramova, S. I.; Santamaria, S.; Cercignani, G.; Marinelli, L.; La Pietra, V.; Novellino, E.; Orlandini, E., Nencetti, S.; Tuccinardi, T.; Martinelli, A.; Lim, N. H.; Visse, R.; Nagase, H.; Rossello, A. N-O-isopropyl sulfonamido-based hydroxamates: design, synthesis and biological evaluation of selective matrix metalloproteinase-13 inhibitors as potential therapeutic agents for osteoarthritis. *J. Med. Chem.* **2009**, *52*, 4757-4773.

(19) a) Nuti, E.; Casalini, F.; Avramova, S. I.; Santamaria, S.; Fabbi, M.; Ferrini, S.; Marinelli, L.; La Pietra, V.; Limongelli, V.; Novellino, E.; Cercignani, G.; Orlandini, E.; Nencetti, S.; Rossello, A. Potent arylsulfonamide inhibitors of tumor necrosis factor-alpha converting enzyme able to reduce activated leukocyte cell adhesion molecule shedding in cancer cell models. *J. Med. Chem.*

2010, *53*, 2622-2635. b) Nuti, E.; Casalini, F.; Santamaria, S.; Fabbi, M.; Carbotti, G.; Ferrini, S.; Marinelli, L.; La Pietra, V.; Novellino, E.; Camodeca, C.; Orlandini, E.; Nencetti, S.; Rossello, A. Selective arylsulfonamide inhibitors of ADAM-17: hit optimization and activity in ovarian cancer cell models. *J. Med. Chem.* **2013**, *56*, 8089-8103.

(20) a) Rossello, A.; Nuti, E.; Orlandini, E.; Carelli, P.; Rapposelli, S.; Macchia, M.; Minutolo, F.; Carbonaro, L.; Albini, A.; Benelli, R.; Cercignani, G.; Murphy, G.; Balsamo, A. New *N*-arylsulfonyl-*N*-alkoxyaminoacetohydroxamic acids as selective inhibitors of gelatinase A (MMP-2). *Bioorg. Med. Chem.* **2004**, *12*, 2441-2450. b) Rossello, A.; Nuti, E.; Orlandini, E.; Balsamo, A.; Tuccinardi, T. Compounds having aryl-sulphonamidic structure useful as metalloproteases inhibitors. PCT WO2008113756, **2008**.

(21) Neumann, U.; Kubota, H.; Frei, K., Ganu, V., Leppert, D. Characterization of Mca-Lys-Pro-Leu-Gly-Leu-Dpa-Ala-Arg-NH_2, a fluorogenic substrate with increased specificity constants for collagenases and tumor necrosis factor converting enzyme. *Anal. Biochem.* **2004**, *328*, 166-173.

(22) Becker, D. P.; Barta, T. E.; Bedell, L. J.; Boehm, T. L.; Bond, B. R.; Carroll, J.; Carron, C. P.; DeCrescenzo, G. A.; Easton, A. M.;Freskos, J. N.; Funckes-Shippy, C. L.; Heron, M.; Hockerman, S.; Howard, C. P.; Kiefer, J. R.; Li, M. H.; Mathis, K. J.; McDonald, J. J.; Mehta, P. P.; Munie, G. E.; Sunyer, T.; Swearingen, C. A.; Villamil, C. I.; Welsch, D.; Williams, J. M.; Yu, Y.; Yao, J. Orally active MMP-1 sparing α-tetrahydropyranyl and α-piperidinyl sulfone matrix metalloproteinase (MMP) inhibitors with efficacy in cancer, arthritis, and cardiovascular disease. *J. Med. Chem.* **2010**, *53*, 6653−6680.

(23) Overall, C. M.; Kleifeld, O. Tumour microenvironment - opinion: validating matrix metalloproteinases as drug targets and anti-targets for cancer therapy. *Nat. Rev. Cancer.* **2006**, *6*, 227-239.

(24) Deryugina, E. I.; Quigley, J. P. Tumor angiogenesis: MMP-mediated induction of intravasation- and metastasis-sustaining neovasculature. *Matrix Biol.* **2015**, *44*, 94-112.

(25) Rossello, A.; Nuti, E. Drug design of sulfonylated MMP inhibitors. In Drug Design of Zinc-Enzyme Inhibitors: Functional, Structural, and Disease Applications; Wiley Series in Drug Discovery and Development; Wang, B., series Ed.; John Wiley & Sons, Inc.: New York, 2009; pp 549-589.

(26) Kawasaki, Y.; Xu, Z. Z.; Wang, X.; Park, J. Y.; Zhuang, Z. Y.; Tan, P. H.; Gao, Y. J.; Roy, K.; Corfas, G.; Lo, E. H.; Ji, R. R. Distinct roles of matrix metalloproteases in the early and late phase development of neuropathic pain. *Nat. Med.* **2008**, *14*, 331-336.

(27) a) Warpehoski, M. A.; Mitchell, M. A.; Jacobsen, E. J. J.; α-Amino sulfonyl hydroxamic acids as metalloproteinase inhibitors. US 5804593, **1998**. b) Subramaniam, R.; Haldar, M. K.; Tobwala, S.; Ganguly, B.; Srivastavab, D. K.; Mallik, S. Novel bis-(arylsulfonamide) hydroxamate-based selective MMP inhibitors. *Bioorg. Med. Chem. Lett.* **2008**, *18*, 3333–3337. c) Jacobsen, E. J. J.; Skaletzky, L. L. Bis-sulfonamides hydroxamic acids as MMP inhibitors. US 5859061, **1999**. d) Ma, D.; Wu, W.; Yang, G.; Li, J.; Li, J.; Ye, Q. Tetrahydroisoquinoline based sulfonamide hydroxamates as potent matrix metalloproteinase inhibitors. *Bioorg. Med. Chem. Lett.* **2004**, *14*, 47–50. e) Cheng, X.C.; Wang, Q.; Fang, H.; Tang, W.; Xu, W. F. Synthesis of new sulfonyl pyrrolidine derivatives as matrix metalloproteinase inhibitors. *Bioorg. Med. Chem.* **2008**, *16*, 7932–7938. f) Hiruma, T; Kobayashi, K; Inomata, S. Azabicyclo compound, matrix metalloprotease inhibitor, and skin preparation. EP1452527, **2002**.

(28) a) Albini, A.; Iwamoto, Y.; Kleinman, H. K.; Martin, G. R.; Aaronson, S. A.; Kozlowski, J. M.; McEwan, R. N. A rapid in vitro assay for quantitating the invasive potential of tumor cells. *Cancer Res.* **1987**, *47*, 3239-3245. b) Albini, A.; Benelli, R. The chemoinvasion assay: a method to assess tumor and endothelial cell invasion and its modulation. *Nat. Protoc.* **2007**, *2*, 504-511.

(29) Albini, A.; Fontanini, G.; Masiello, L.; Tacchetti, C.; Bigini, D.; Luzzi, P.; Noonan, D. M.; Stetler-Stevenson, W. G. Angiogenic potential in vivo by Kaposi's sarcoma cell-free supernatants

and HIV-1 tat product: inhibition of KS-like lesions by tissue inhibitor of metalloproteinase-2. *AIDS.* **1994**, *8*, 1237-1244.

(30) SoftMax Pro 4.7.1 by Molecular Devices.

(31) GraFit version 4 by Erithecus Software.

(32) Carpentier, G. Contribution: Angiogenesis Analyzer. ImageJ News. 2012.

(33) Rozen, S.; Skaletsky, H. Primer3 on the WWW for general users and for biologist programmers. *Methods Mol. Biol.* **2000**, *132*, 365-386.

(34) Berman, H. M.; Westbrook, J.; Feng, Z.; Gilliland, G.; Bhat, T. N.; Weissig, H.; Shindyalov, I. N.; Bourne, P. E. The Protein Data Bank. *Nucleic Acids Res.* **2000**, *28*, 235-242.

(35) Case, D. A.; Darden, T. A.; III, T. E. C.; Simmerling, C. L.; Wang, J.; Duke, R. E.; Luo, R.; Walker, R. C.; Zhang, W.; Merz, K. M.; Roberts, B.; Wang, B.; Hayik, S.; Roitberg, A.; Seabra, G.; Kolossváry, I.; Wong, K. F.; Paesani, F.; Vanicek, J.; Liu, J.; Wu, X.; Brozell, S. R.; Steinbrecher, T.; Gohlke, H.; Cai, Q.; Ye, X.; Wang, J.; Hsieh, M.-J.; Cui, G.; Roe, D. R.; Mathews, D. H.; Seetin, M. G.; Sagui, C.; Babin, V.; Luchko, T.; Gusarov, S.; Kovalenko, A.; Kollman, P. A. *AMBER*, version 11; in University of California: San Francisco, CA, 2010.

(36) Morris, G. M.; Goodsell, D. S.; Halliday, R. S.; Huey, R.; Hart, W. E.; Belew, R. K.; Olson, A. J. Automated docking using a Lamarckian genetic algorithm and an empirical binding free energy function. *J. Comput. Chem.* **1998**, *19*, 1639-1662.

(37) Morris, G. M.; Huey, R.; Lindstrom, W.; Sanner, M. F.; Belew, R. K.; Goodsell, D. S.; Olson, A. J. AutoDock4 and AutoDockTools4: Automated docking with selective receptor flexibility. *J. Comput. Chem.* **2009**, *30*, 2785-2791.

(38) York, D. M.; Darden, T. A.; Pedersen, L. G. The effect of long range electrostatic interactions in simulations of macromolecular crystals: a comparison of the Ewald and truncated list methods. *J. Chem. Phys.* **1993**, *99*, 8345–8348.

(39) Vera, L.; Antoni, C.; Devel, L.; Czarny, B.; Cassar-Lajeunesse, E.; Rossello, A.; Dive, V.; Stura, E. A. Screening Using Polymorphs for the Crystallization of Protein–Ligand Complexes. *Cryst. Growth Des.* **2013**, *13*, 1878-1888.

(40) Vera, L.; Stura, E. A. Strategies for Protein Cryocrystallography. *Cryst. Growth Des.* **2014**, *14*, 427–435.

(41) Kabsch, W. XDS. *Acta Crystallogr. D. Biol. Crystallogr.* **2010**, *66*, 125–132.

(42) Murshudov, G. N.; Skubák, P.; Lebedev, A. A.; Pannu, N. S.; Steiner, R. A.; Nicholls, R. A.; Winn, M.D.; Long, F.; Vagin, A. A. REFMAC5 for the refinement of macromolecular crystal structures. *Acta Crystallogr. D. Biol. Crystallogr.* **2011**, *67*, 355–367.

(43) Winn, M. D.; Ballard, C. C.; Cowtan, K. D.; Dodson, E. J.; Emsley, P.; Evans, P. R.; Keegan, R. M.; Krissinel, E. B.; Leslie, A. G. W.; McCoy, A.; McNicholas, S. J.; Murshudov, G. N.; Pannu, N. S.; Potterton, E. A.; Powell, H. R.; Read, R. J.; Vagin, A.; Wilson, K. S. Overview of the CCP4 suite and current developments. *Acta Crystallogr. D. Biol. Crystallogr.* **2011**, *67*, 235–242.

(44) Emsley, P.; Lohkamp, B.; Scott, W. G.; Cowtan, K. Features and development of Coot. *Acta Crystallogr. D. Biol. Crystallogr.* **2010**, *66*, 486–501.

(45) Adams, P. D.; Afonine, P. V.; Bunkóczi, G.; Chen, V. B.; Davis, I. W.; Echols, N.; Headd, J. J.; Hung, L.-W.; Kapral, G. J.; Grosse-Kunstleve, R. W.; McCoy, A. J.; Moriarty, N. W.; Oeffner, R.; Read, R. J.; Richardson, D. C.; Richardson, J. S.; Terwilliger, T.C.; Zwart, P. H. PHENIX: a comprehensive Python-based system for macromolecular structure solution. *Acta Crystallogr. D. Biol. Crystallogr.* **2010**, *66*, 213–221.

(46) Stura, E. A., Wilson, I. A. Applications of the streak seeding technique in protein crystallization. *J. Cryst. Growth* **1991**, *110*, 270–282.

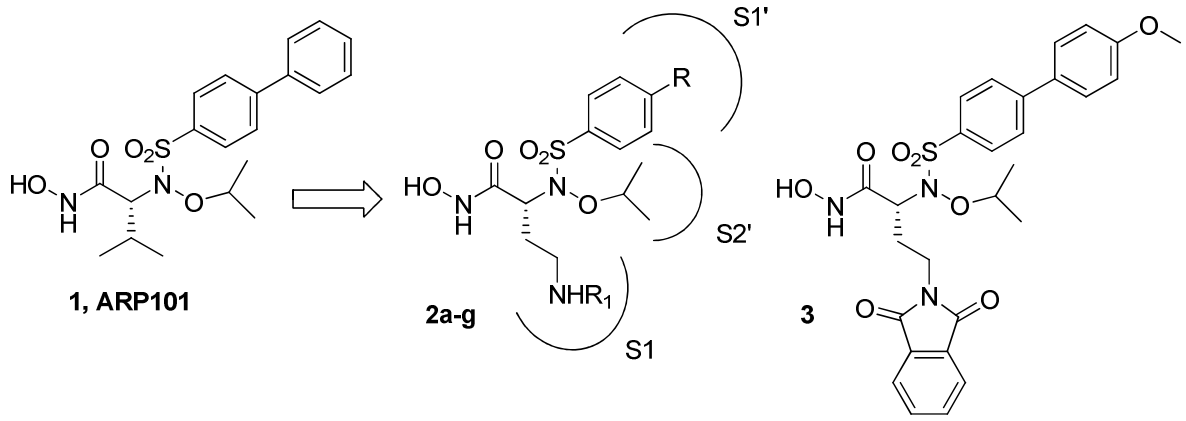

Figure 1.

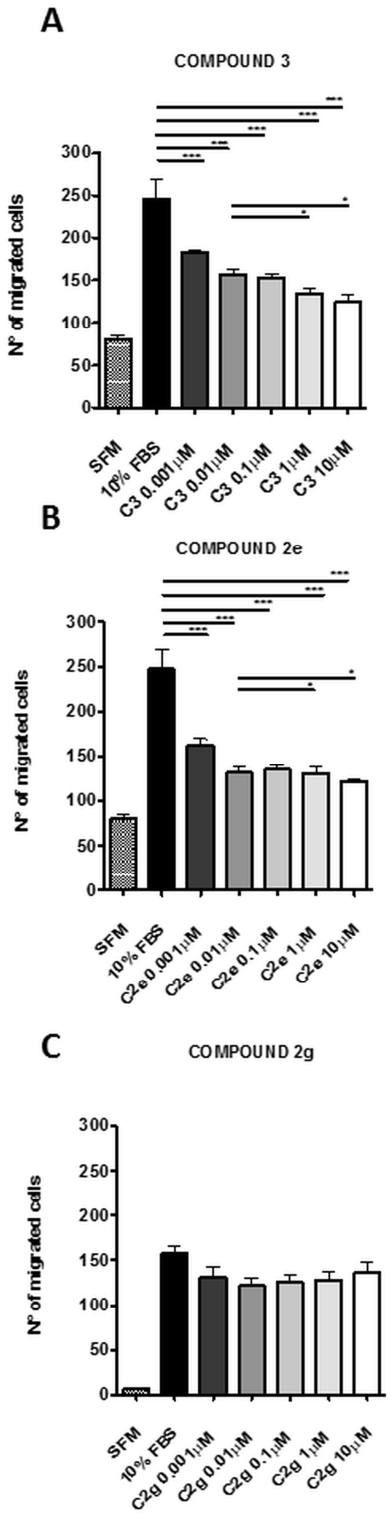
A
COMPOUND 3
N° of migrated cells
300
250
200
150
100
50
0
SFM
10% FBS
C3 0.001µM
C3 0.01µM
C3 0.1µM
C3 1µM
C3 10µM
B
COMPOUND 2e
N° of migrated cells
SFM
10% FBS
C2e 0.001µM
C2e 0.01µM
C2e 0.1µM
C2e 1µM
C2e 10µM
C
COMPOUND 2g
N° of migrated cells
SFM
10% FBS
C2g 0.001µM
C2g 0.01µM
C2g 0.1µM
C2g 1µM
C2g 10µM

Figure 2.

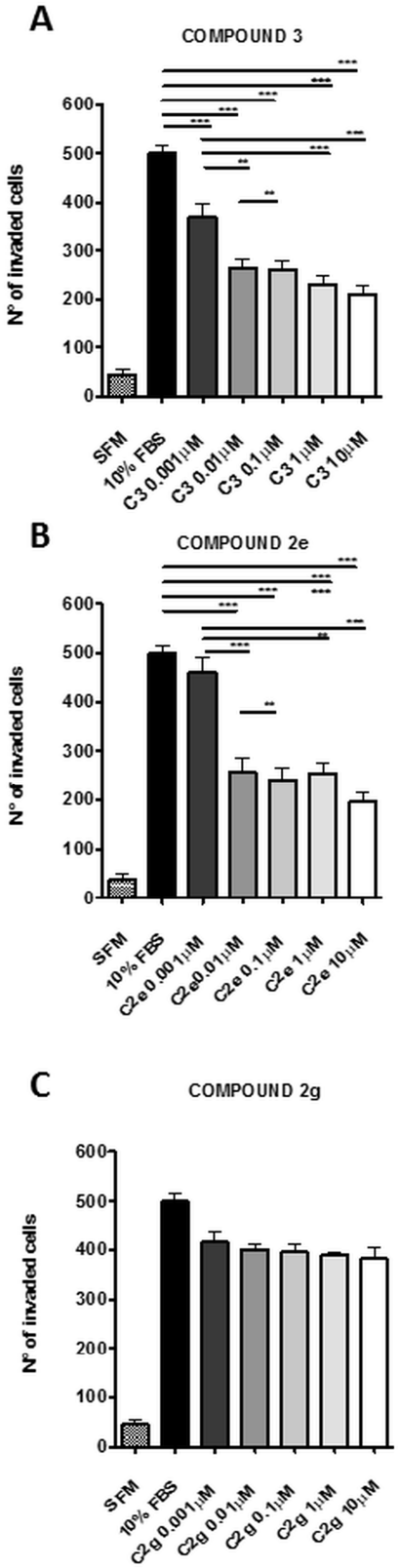
A
COMPOUND 3
N° of invaded cells
600
500
400
300
200
100
0
SFM
10% FBS
C3 0.001µM
C3 0.01µM
C3 0.1µM
C3 1µM
C3 10µM
B
COMPOUND 2e
N° of invaded cells
SFM
10% FBS
C2e 0.001µM
C2e0.01µM
C2e 0.1µM
C2e 1µM
C2e 10µM
C
COMPOUND 2g
N° of invaded cells
SFM
10% FBS
C2g 0.001µM
C2g 0.01µM
C2g 0.1µM
C2g 1µM
C2g 10µM

Figure 3.

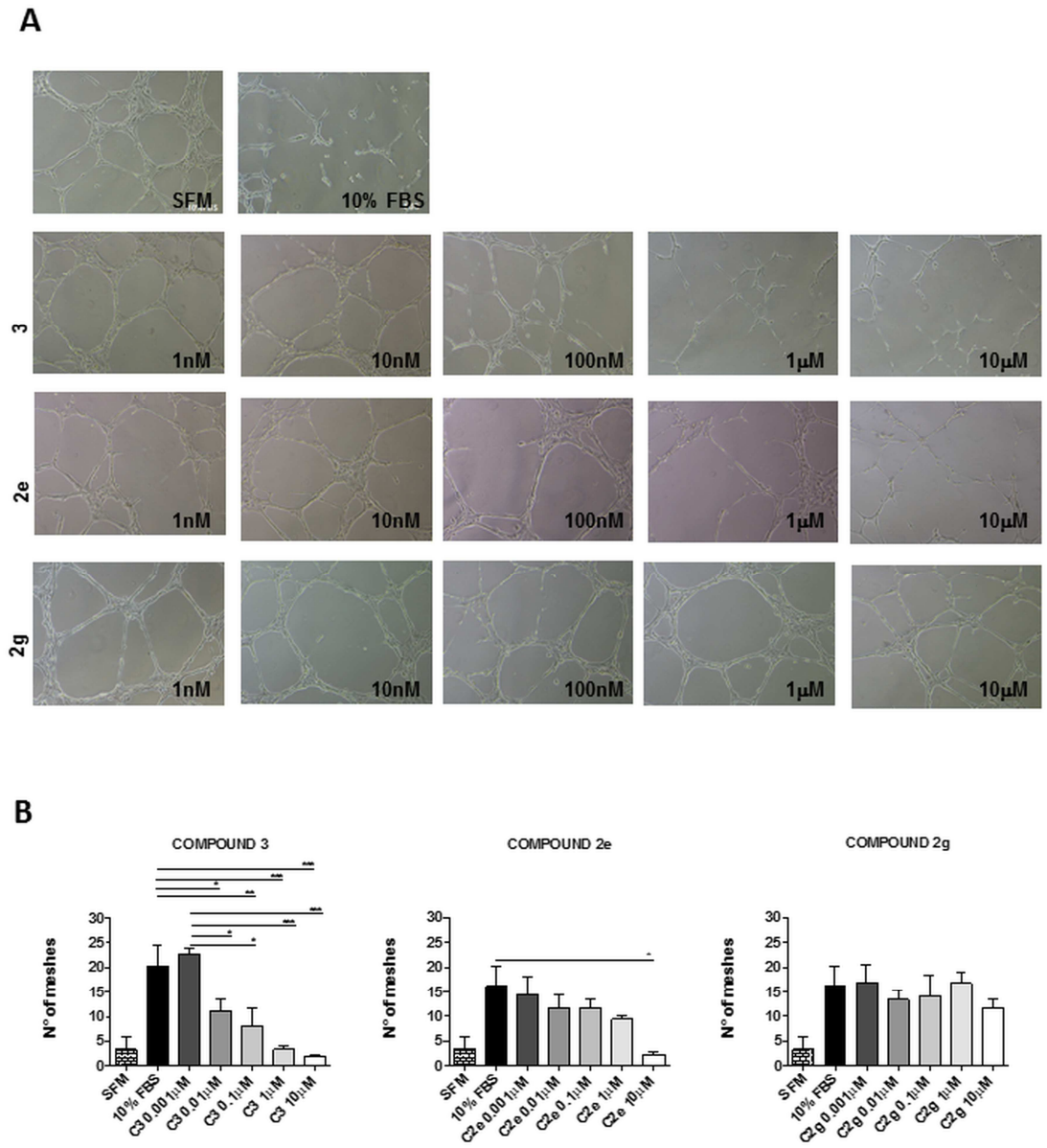
A
SFM
10% FBS
3
1nM
10nM
100nM
1µM
10µM
2e
1nM
10nM
100nM
1µM
10µM
2g
1nM
10nM
100nM
1µM
10µM
B
COMPOUND 3
N° of meshes
SFM
10% FBS
C3 0.001µM
C3 0.01µM
C3 0.1µM
C3 1µM
C3 10µM
COMPOUND 2e
N° of meshes
SFM
10% FBS
C2e 0.001µM
C2e 0.01µM
C2e 0.1µM
C2e 1µM
C2e 10µM
COMPOUND 2g
N° of meshes
SFM
10% FBS
C2g 0.001µM
C2g 0.01µM
C2g 0.1µM
C2g 1µM
C2g 10µM

Figure 4.

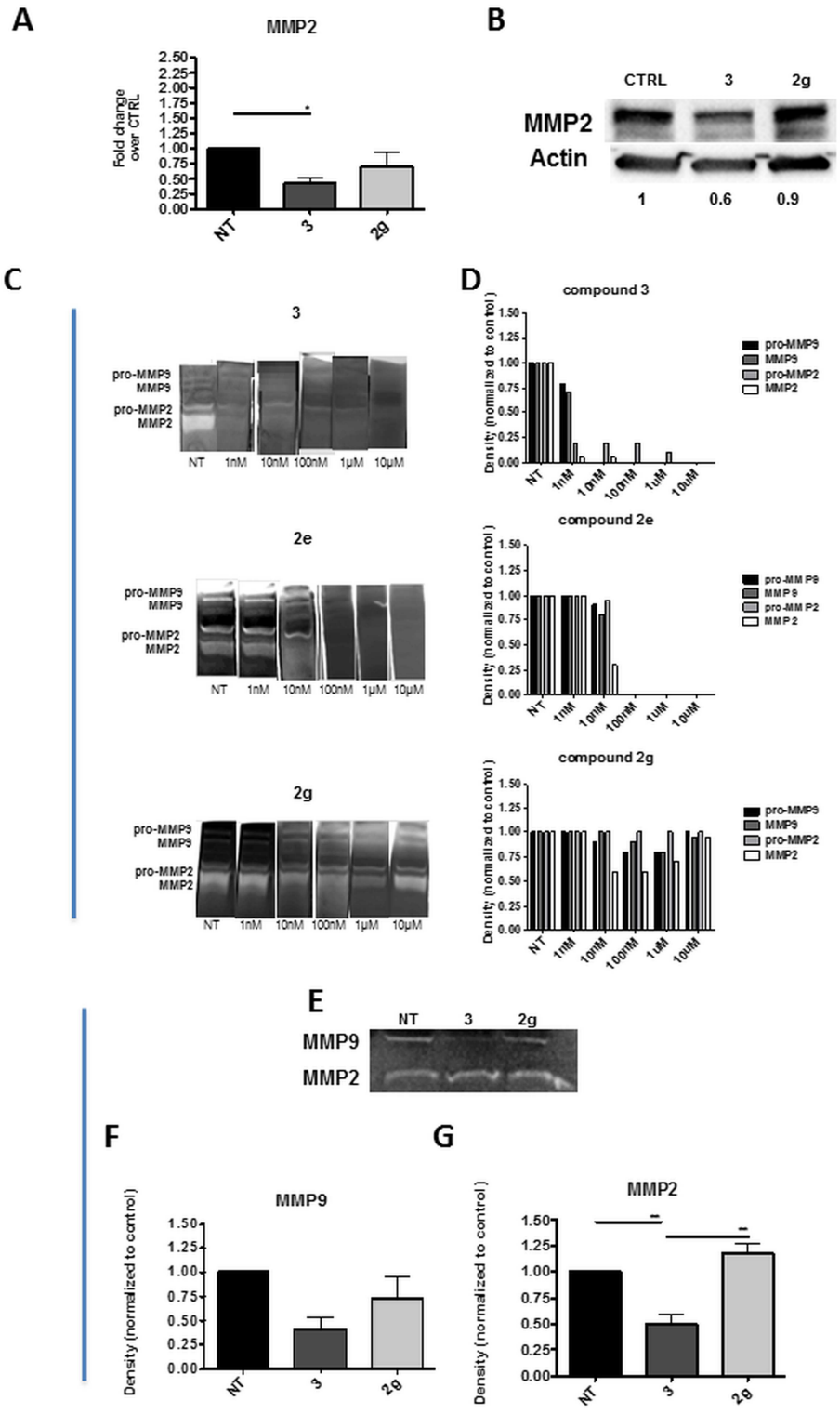
A
MMP2
Fold change over CTRL
2.50
2.25
2.00
1.75
1.50
1.25
1.00
0.75
0.50
0.25
0.00
NT
3
2g
B
CTRL
3
2g
MMP2
Actin
1
0.6
0.9
C
3
pro-MMP9
MMP9
pro-MMP2
MMP2
NT
1nM
10nM
100nM
1µM
10µM
2e
2g
D
compound 3
compound 2e
compound 2g
Density (normalized to control)
pro-MMP9
MMP9
pro-MMP2
MMP2
E
NT
3
2g
MMP9
MMP2
F
MMP9
Density (normalized to control)
G
MMP2
Density (normalized to control)

Figure 5.

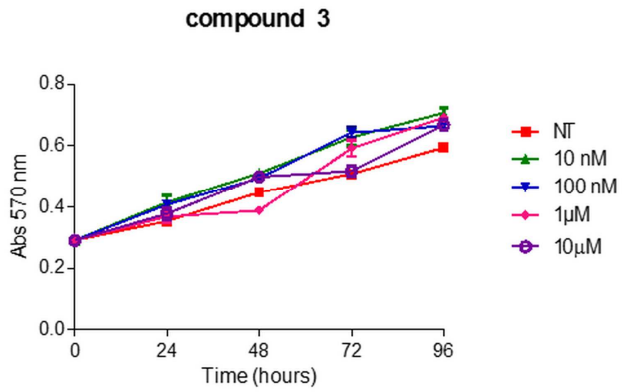

Figure 6.

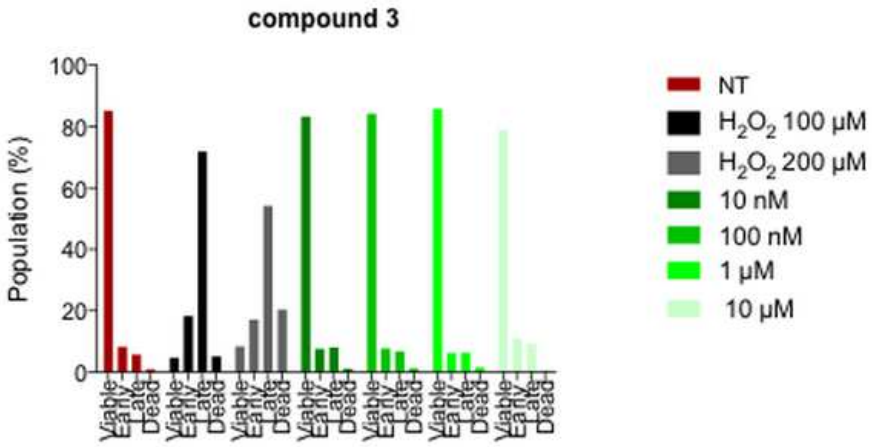

Figure 7.

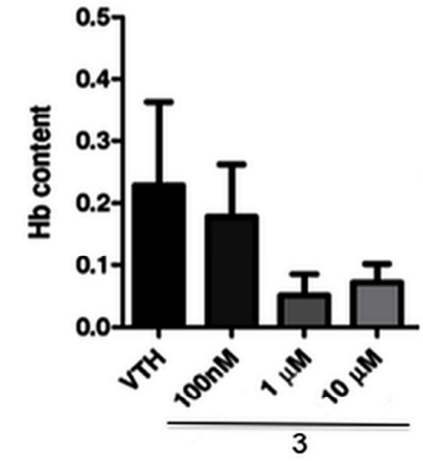
Hb content
0.5
0.4
0.3
0.2
0.1
0.0
VTH
100nM
1 µM
10 µM
3

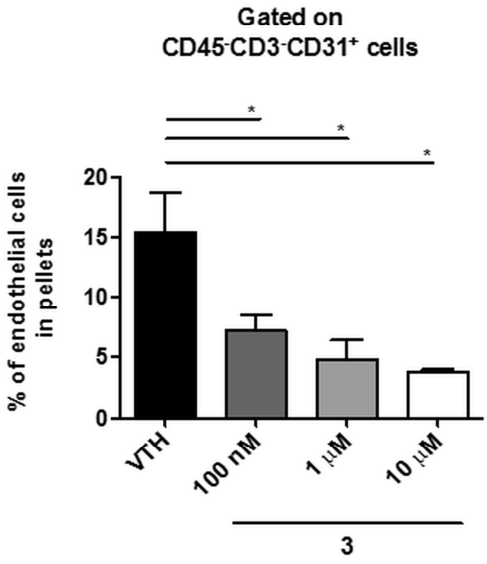
Gated on
CD45-CD3-CD31+ cells
% of endothelial cells in pellets
20
15
10
5
0
*
*
*
VTH
100 nM
1 µM
10 µM
3

Figure 8.

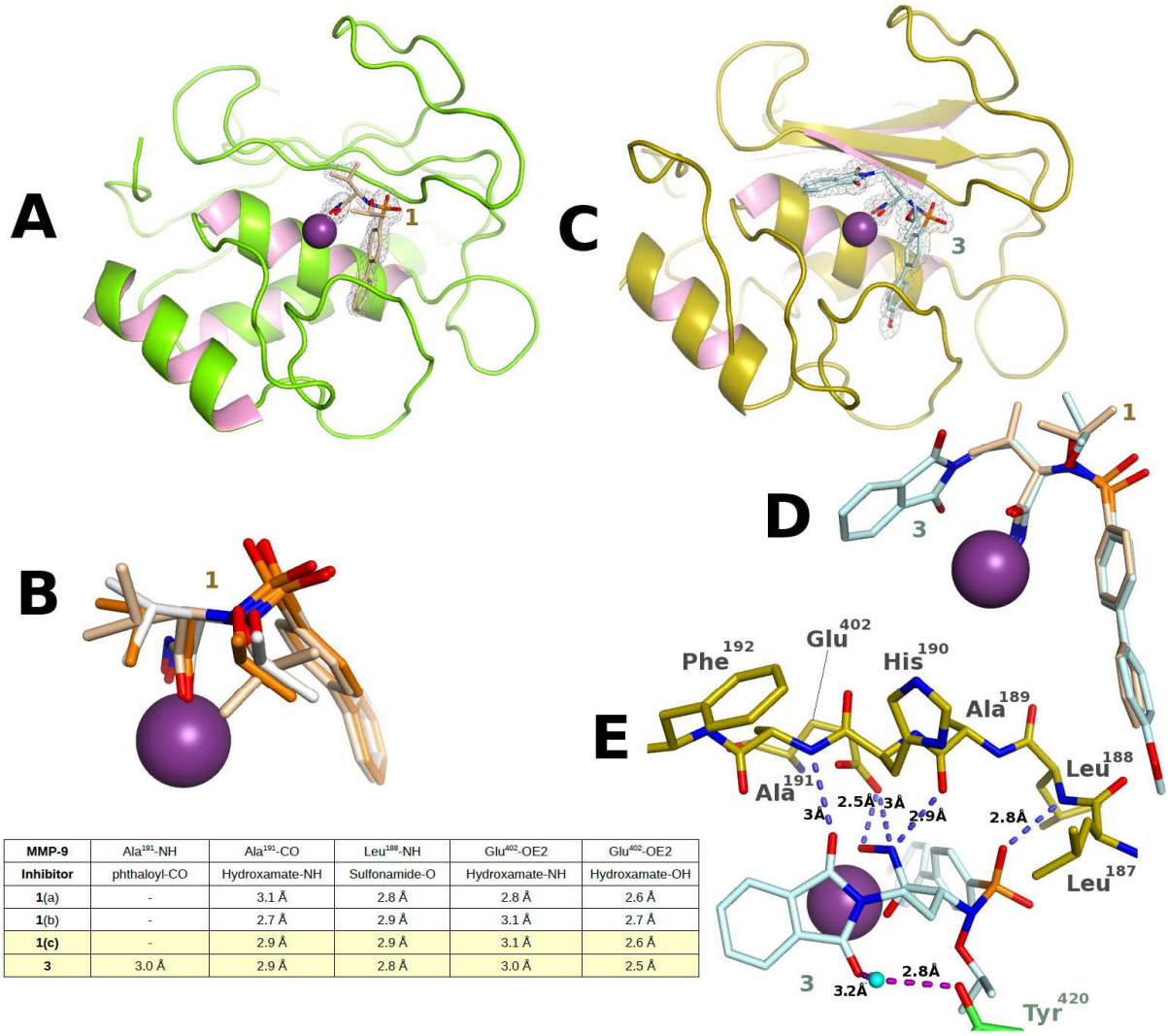

MMP-9	Ala[191]-NH	Ala[191]-CO	Leu[188]-NH	Glu[402]-OE2	Glu[402]-OE2
Inhibitor	phthaloyl-CO	Hydroxamate-NH	Sulfonamide-O	Hydroxamate-NH	Hydroxamate-OH
1(a)	-	3.1 Å	2.8 Å	2.8 Å	2.6 Å
1(b)	-	2.7 Å	2.9 Å	3.1 Å	2.7 Å
1(c)	-	2.9 Å	2.9 Å	3.1 Å	2.6 Å
3	3.0 Å	2.9 Å	2.8 Å	3.0 Å	2.5 Å

Figure 9.

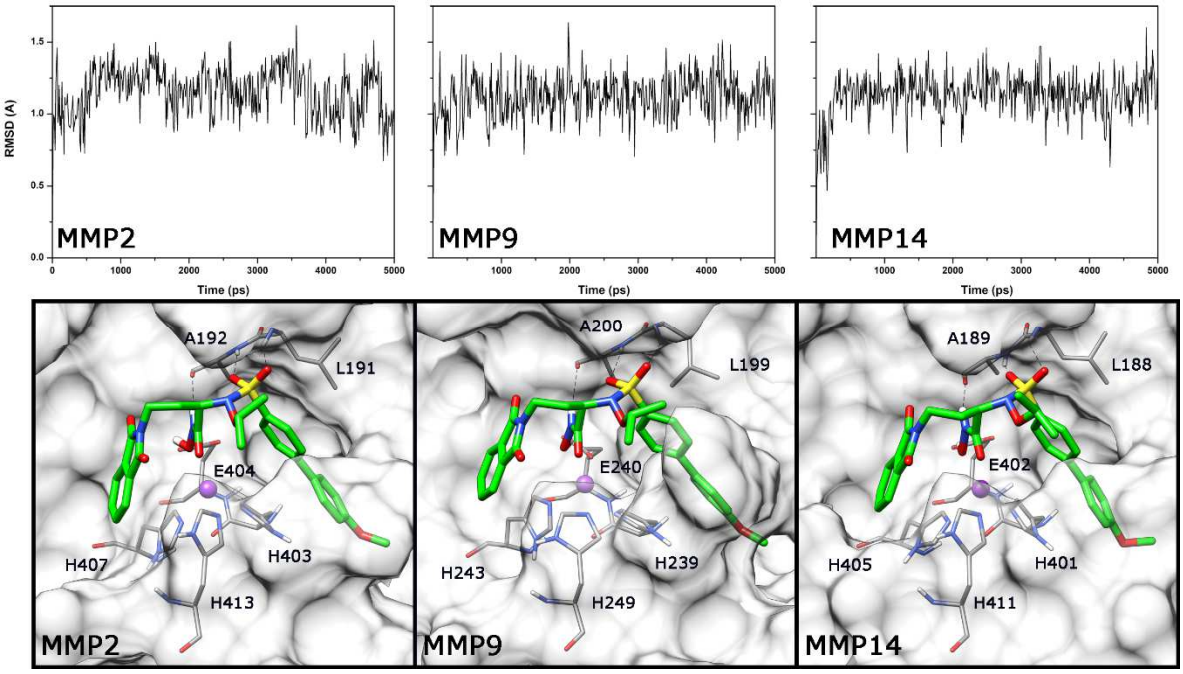

Figure 10.

Figure Captions

Figure 1: Progression of the SAR: from the reference compound **1** to the antiangiogenic agents **2a-g** and **3**.

Figure 2: Effect of MMP inhibitors 2e and 3 on endothelial cell migration in comparison with 2g. In the migration assay, HUVECs were seeded into the upper compartment of Boyden chambers in the presence or absence of inhibitors, whereas 10% FBS was used as chemoattractant were placed in the lower compartment. After 6 h incubation, cells in the upper side of the filter were removed, and cells that migrated to the lower surface were fixed, stained and counted. Serum-free medium (SFM) was used as negative control. All experiments were performed in triplicate and repeated two times. Means ± SEM are shown (***$p<0.001$,* $p<0.05$).

Figure 3: Effect of MMP inhibitors 2e and 3 on endothelial cell invasion in comparison with 2g. The assay was performed in modified Boyden chambers, as described previously[28]. HUVECs (5×10^4) were washed with PBS, resuspended in serum-free medium in the presence or absence of

inhibitors and placed in the upper compartment. Chemoattractant (10% FBS) was added in the lower compartment. Pore-size polycarbonate filters (8 μm) were pre-coated with matrigel (1 mg/mL). After overnight incubation, the filters were recovered, cells on the upper surface mechanically removed and cells invaded the lower filter surface fixed, stained and counted. All experiments were performed in triplicate and repeated two times. Means ± SEM are shown (***P<0.001, **p<0.01).

Figure 4: Effect of MMP inhibitors 2e and 3 on endothelial morphogenesis *in vitro* in comparison with 2g. HUVECs were seeded on the top of the matrigel layer previously polymerized number of mashes on 24-well plates in presence of the indicated concentrations of inhibitors. The formation of capillary-like networks was documented by photography after 6 h (5x magnification, **A**) and number of meshes (**B**), as an indicator of HUVEC tubulogenic efficiency, was determined using the Angiogenesis Analyzer tool, provide by ImageJ (***P<0.001, **p<0.01, *p<0.05).

Figure 5: Effect of 2e and 3 on MMP-2 and MMP-9 activity of endothelial cells in comparison with 2g. A: qPCR analysis for MMP-2 on **3** and **2g** treated HUVECs Vs control; **B**: WB analysis on MMP-2 production on **3** and **2g** treated HUVECs. **C-D**: Representative zymograms showing gelatinase activity of the indicated enzymes on HUVEC conditioned media (CM) subsequently exposed to **3**, **2e** and **2g**; **E**: Representative zymograms showing gelatinase activity of the indicated enzymes on CM derived from **3** and **2g** treated HUVECs. White bands on dark background correspond to enzymed-digested regions. MMP-9 and MMP-2 were identified as their pro- and active forms; **F-G:** Densitometric analysis of zymograms showing relative gelatinase activity.

Figure 6: Effect of 3 on endothelial cell viability. Cell proliferation was evaluated at fixed times (24, 48, 72, 96 h) after the addition of compound **3** to the medium. NT: vehicle; DMSO. Means ± SEM are shown.

Figure 7: Effect of 3 on endothelial cell apoptosis. In the apoptosis assay, HUVECs were treated with increasing concentrations of compound **3**. Vehicle (DMSO; NT) and hydrogen peroxide (H_2O_2) were used as controls. After 18h, cells were recovered, washed and stained with two markers, Annexin V and 7-amino-actinomycin D, used to detect viable, dead or cells undergoing apoptosis. The experiment was performed two times and each condition was in duplicate.

Figure 8: Effect of 3 on angiogenesis *in vivo*. A cocktail of pro angiogenic factors (VEGF-A, TNFα and heparin), either alone (VTH) or in combination with different concentrations of compound **3** as indicated, was added into matrigel and injected subcutaneously into C57/BL6 mice. Drabkin's assay showed decreased hemoglobin content in excised plug from treat mice as compared to those from untreated (**A**). Pellets excised form mice treated with **3** at indicated doses, showed a significantly (*$p<0.05$) decreased number of $CD31^+$ endothelial cells, as compared to controls (**B**).

Figure 9. Schematic representation of the crystal structures of the MMP-9 catalytic domain bound to inhibitors 1 and 3. (A) Overall fold of the catalytic domain with **1** (PDB accession code: 4XCT) in ochre and the catalytic zinc in purple, with the experimental electron density for the ligand (weighted 2Fo-Fc). **(B)** The three polymorphs provide valuable information about the variability in ligand positioning limited to positional variations of the propyl and oxypropyl moieties. **(C)** Electron density for **3** in complex with MMP9 (PDB accession code: 4WZV). **(D)** Variability in the sulfur oxygen positioning between **1** and **3** is noted. The distances are given in the insert. **(E)** An additional direct hydrogen bond is observed between the phthaloyl carboxyl of **3** and the amide nitrogen of Ala 191; in the complex with **1** it is replaced by an interaction with a water molecule.

Figure 10. Analysis of the MD simulation of **3** complexed with MMP-2, MMP-9, and MMP-14. RMSD analysis of the ligand from the starting model structure during the simulations (upper) and minimized average structures of **3** docked into MMP-2, MMP-9 and MMP-14 (lower). PDB codes of the starting MMP-2, MMP-9, and MMP-14 crystal structures are 1QIB, 4WZV, and 3MA2.

Table 1. *In vitro*[a] activity (IC_{50}, nM) of *N*-isopropoxy-arylsulfonamide hydroxamates **2a-g**, **3** and the reference compound **1** on MMPs.

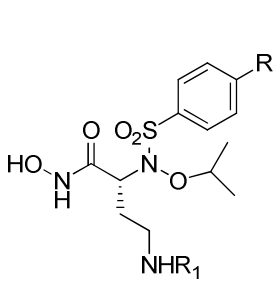

2a-g

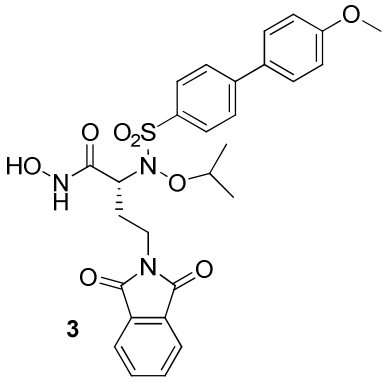

3

Compd	R	R_1	MMP-1	MMP-2	MMP-3	MMP-9	MMP-13	MMP-14
2a	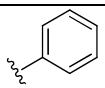	-COPh	780	1.5	450	9.0	4.6	94
2b		$-SO_2CH_3$	320	1.0	71	8.6	2.2	95
2c		$-COCH_3$	280	0.33	47	6.5	0.68	41
2d		-COBn	1300	1.4	120	6.4	1.4	81
2e	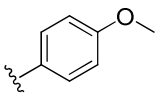	$-COCH_3$	660	0.13	20	2.0	0.58	23
2f	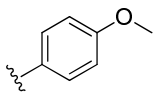	-COBn	1400	0.37	36	2.9	0.25	25
2g	H	$-COCH_3$	26000	590	-	3900	1800	5500
3			200	0.67	105	0.43	0.19	3.9
1[18]			490	0.81	50	6.7	4.1	9.8

[a]Enzymatic data are mean values for three independent experiments performed in duplicate. SD were generally within ±10%.

Scheme 1. Synthesis of *N*-isopropoxy-arylsulfonamide hydroxamates **2a-g**[a]

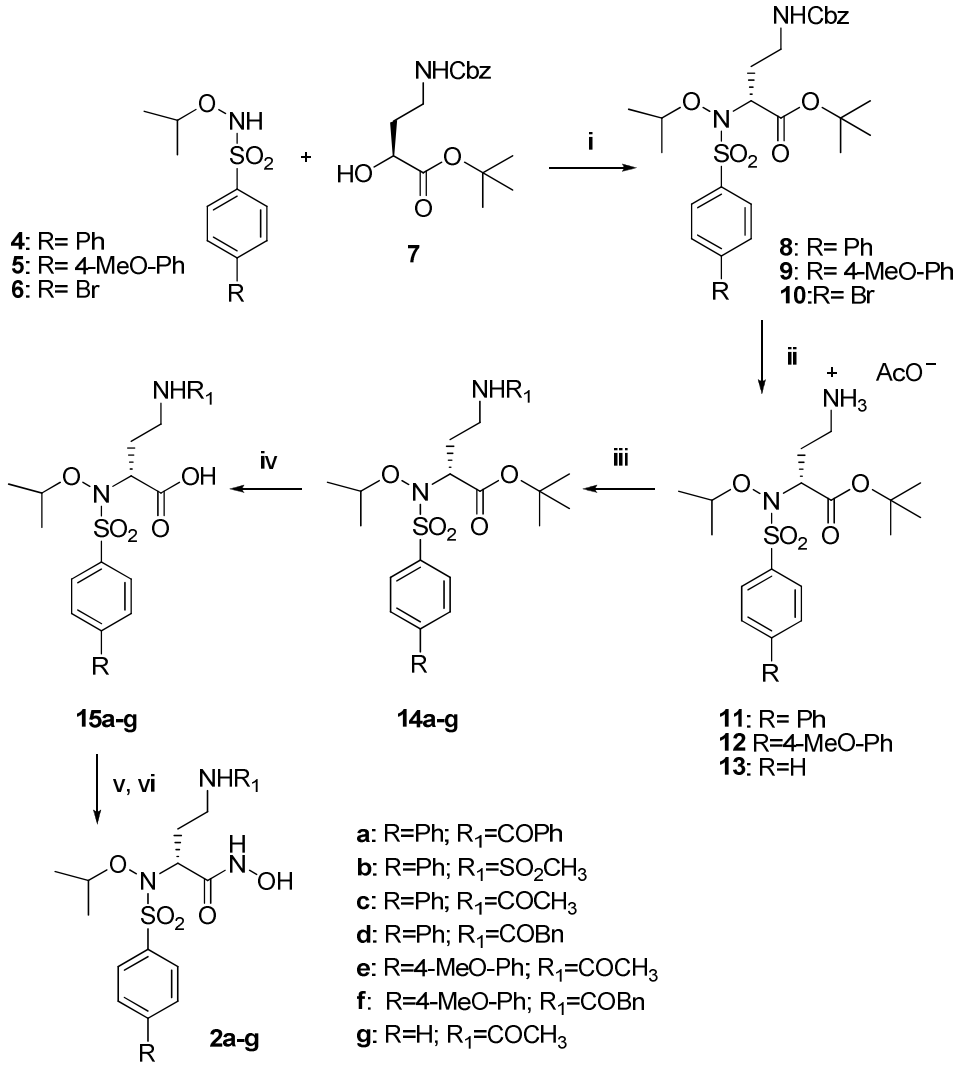

[a] Reagents and conditions: (i) PPh_3, DIAD, THF; (ii) H_2, Pd/C 10%, AcOH, MeOH; (iii) R_1Cl, DIPEA, DMF; (iv) TFA, CH_2Cl_2, 0 °C; (v) $TBDMSiONH_2$, EDC, CH_2Cl_2; (vi) TFA, CH_2Cl_2, 0 °C.

Scheme 2. Synthesis of *N*-isopropoxy-4-methoxybiphenylsulfonamide hydroxamate **3**[a]

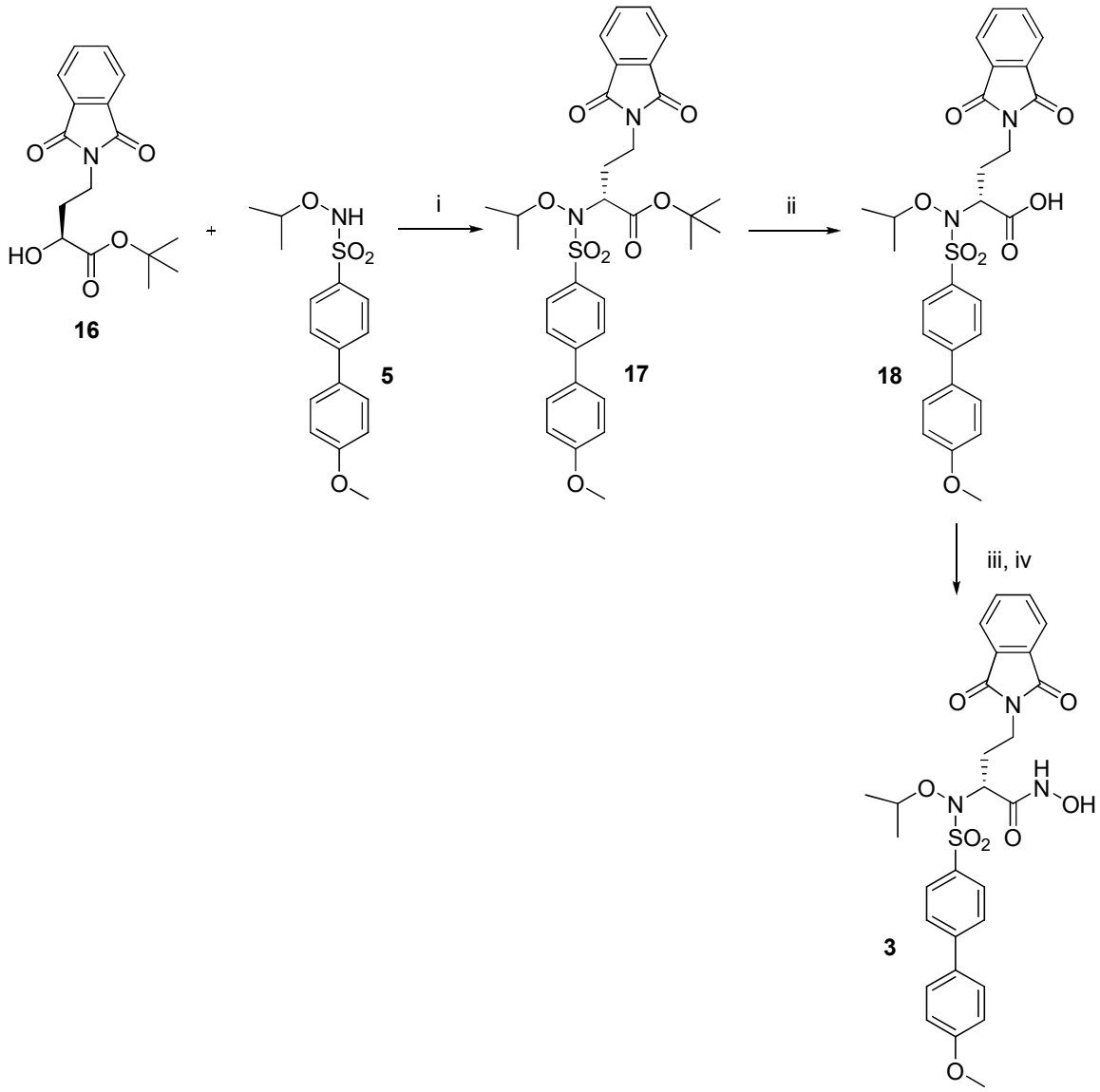

[a] Reagents and conditions: (i) PPh_3, DIAD, THF; (ii) TFA, CH_2Cl_2, 0 °C; (iii) $TBDMSiONH_2$, EDC, CH_2Cl_2; (iv) TFA, CH_2Cl_2, 0 °C.

Table of Contents Graphic